The Young's modulus of compression-moulded LLDPE-phlogopite composites

CJR Verbeek
Department of Chemical Engineering
University of Pretoria

The Young's modulus of compression-moulded LLDPE-phlogopite composites

CJR Verbeek
Department of Chemical Engineering
University of Pretoria

Submitted in partial fulfilment of the degree Philosophiae Doctor in the Faculty of Engineering, Built Environment and Information Technology, University of Pretoria, Pretoria.

Supervisor:

Professor W.W. Focke

October 2001

To Petra

The Young's modulus of compression-moulded LLDPE-phlogopite composites

by

Casparus Johannes Reinhard Verbeek

Supervisor

Prof. W.W. Focke

Department of Chemical Engineering

for the degree Philosophiae Doctor

Particulate reinforced polymers is a mature field and many models are available to predict the Young's modulus of such composites. However, all the existing models have a common flaw; they all predict that the composite modulus equals that of the reinforcing agent when the polymer content approaches zero. This implies, in this limit, a monolithic reinforcement whereas, in fact, it is composed of discrete particles with very little interaction. This is a serious drawback and therefore this study focussed on:

- finding the composition and processing variables that contribute most to the Young's modulus of a LLDPE / phlogopite composite and
- deriving an improved model for the Young's modulus in the plane of the reinforcement.

The Taguchi method was used to separately investigate the effects of composition and processing variables on the mechanical properties of compression moulded sheets. The composition variables considered were: particle size, polymer content and type of polymer modification. With respect to main effects (Young's Modulus) the factors particle size and polymer content were found to be the most important. It should, however, be noted that the modulus showed a broad maximum in the range of polymer content investigated. This could have masked the true effect of binder content.

The processing variables considered were: holding pressure, mould temperature, moulding time and the amount of material moulded per unit area. Concerning the preparation variables, pressure contributed the most towards the Young's modulus, although the contribution was small. The experimental results for the flexural modulus confirmed that pressure was the most important preparation variable. Particle shape will ultimately influence the ability for good packing of particles in the composite. Poor packing will result in a high voidage, especially when the polymer content is low. Using a high holding pressure helps to reduce this voidage.

The voidage of the present samples were correlated with the volume fraction binder and the maximum packing density of the pure reinforcement. A theoretical model was derived along the lines of the Padawer-and-Beecher-modified-Cox model. However, it included the effect of composite voidage on the composite's mechanical properties. In contrast to other available models, it correctly predicts the loss of material stiffness and strength in the limit of zero binder content.

Keywords:

Polyethylene, phlogopite, Young's modulus, voidage, packing platelet, reinforcing agent, binder, aspect ratio, model

SINOPSIS

Young se modulus vir persgietgevormde LLDPE-flogopiet samestellings

deur

Casparus Johannes Reinhard Verbeek

Promotor

Prof. W.W. Focke

Departement Chemiesè Ingenieurswese

vir die graad Philisophiae Doctor

Partikel-versterkte polimere is 'n gevestigde veld en verskeie modelle is beskikbaar om Young se modulus te voorspel. Al die bestaande modelle het egter een gemeenskaplike nadeel; dit is dat hierdie modelle voorspel dat Young se modulus gelyk is aan die partikel materiaal-modulus wanneer die polimeerinhoud neig na nul. Dit impliseer, in hierdie limiet, dat die versterker kontinu is, terwyl dit egter uit diskrete partikels bestaan met baie min interaksie. Dit is 'n ernstige nadeel en hierdie studie het daarom gefokus op:

- die bepaling van die samestelling- en prosesseringsveranderlikkes wat die meeste bydra tot Young se modulus van sulke materiale
- die afleiding van 'n verbeterde model om Young se modulus te voorspel in die vlak van oriëntasie van die versterker.

Die Taguchi metode is gebruik om onderskeidelik die invloed van die samestellingveranderlikes en

prosesseringsveranderlikes te bepaal op die meganiese eienskappe van persgietgevormde velle. Die samestellingsveranderlikes ondersoek was: partikel grootte, polimeerinhoud en tipe polimeer modifikasie. Met betrekking tot die hoof effek (Young se modulus) is daar gevind dat partikkel groote en polimeerinhoud die belangrikste faktore was. Daar moet egter in gedagte gehou word dat die modulus 'n breë maksimum toon in die gebied van polimeerinhoud wat ondersoek is. Dit kon dalk die ware effek van polimeerinhoud verskuil.

Die prosesseringsveranderlikkes ondersoek was: prosseseringsdruk, vormingstyd, en die hoeveelheid materiaal gebruik per eenheidsarea. Met betrekking tot die prosesseringsveranderlikkes dra prosseseringsdruk die meeste by tot Young se modulus, maar, die effek is klein in vergelyking met die foutterm. Die eksperimentele resultate vir buigmodulus het egter bevestig dat prosesseringsdruk die belangrikste prosseseringsveranderlikke is. Verder, beïnvloed partikelvorm ook die vermoë van die partikels om dig te pak. Swak pakking veroorsaak 'n hoë porositeit in die materiaal, veral as daar min polimeer teenwoordig is. Toepassing van 'n hoë prosseseringsdruk verlaag die porositeit.

Die porositeit van die materiaal hier tersprake, is gekorreleer met die volumefraksie polimeer en die maksimum pakkingsdigtheid van die suiwer versterkingsmateriaal. 'n Teoretiese model, gebasseer op die van Cox, soos gemodifiseer deur Padawer en Beecher, is afgelei om Young se modulus te voorpel. Die nuwe model sluit egter die effek van porositeit, op die meganiese eienskappe van die materiaal, in. In kontras met die ander modelle voorspel hierdie materiaal die verlies in materiaal styfheid en sterkte, die korrekte gedrag by die limiet geval van geen polimeer teenwoordig.

Sleutelwoorde:

Poliëtileen, flogopiet, Young se modulus, porositeit, pakking, plaatjie, versterkingsmateriaal, binder, aspekverhouding, model

ACKNOWLEDGEMENTS

I wish to thank:

- Prof. W.W. Focke for guidance and supervision
- Dr. G. van der Linde for making this project possible
- Foskor and the THRIP programme of the NRF and the Department of Trade and Industry for funding the project
- Petra, for your unconditional support during the project

Contents

LIST OF SYMBOLS

A_c	Area of the composite over which the tensile force acts
A_f	Area of a particle
A_p	Area of the polymer over which the tensile force acts
A_{pa}	Particle area
A_v	Void area
D	Particle length
E_c	Young's modulus of the composite in the plane of orientation
E_m	Young's modulus of the reinforcement (mica)
E_p	Young's modulus of the polymer
F_c	Tensile force acting on the composite
F_m	Average tensile force acting on the platelet
F_p	Tensile force acting on polymer
G_p	Shear modulus of the polymer
MRF	Modulus reduction factor
S	Spacing between plates
t	Plate thickness (m)
u	Displacement of the particle at distance x from the edge
v	Displacement of the polymer at distance x, form the edge of the particle when no particles are present
$V_{apparent}$	Apparent volume of one particle (m^3)
v_f	Volume fraction reinforcement, associated with zero voidage
v'_f	True volume fraction reinforcement
$v_{f,max}$	Maximum true volume fraction filler

v_p	Volume fraction polymer, associated with zero voidage
v'_p	True volume fraction polymer
$V_{particle}$	Volume of one particle (m^3)
W	Width of the plates
x_m	Mass fraction filler
x_p	Mass fraction polymer
y	Constant used in the Hirsch model to determine the contribution of the different mixing rules (Equation 2).
α	Flake aspect ratio
γ	Shear strain
$\rho_{composite}$	Measured density of the composite (kg/m^3)
ρ_m	Filler density
ρ_p	Polymer density
$\rho_{theoretical}$	Density of the composite based on zero voidage (kg/m^3)
σ_c	Tensile stress in the composite
$\sigma_f(x)$	The tensile stress in the particle as a function on the position along the particle
σ_p	Tensile stress in the polymer
τ	Shear stress
ϕ	Voidage
ϕ_d	Voidage caused by debonding
ϕ_m	Fraction void volume per cubic metre particles
$\phi_{m,max}$	Maximum void volume based on 1 m^3 when no polymer is present (m^3)
χ	Modified voidage (Voidage relative to polymer phase)
ν_{ps}	Poison's ratio of the polymer
ω	Restricted displacement of the polymer due to the filler
ε	Strain in the composite

Definitions:

ANOVA	Analysis of variance. Used to investigate the relative contribution of various factors on the main effect.
Binder	Polymer phase in the composite. If the volume fraction binder becomes more significant it is also referred to as the matrix
LLDPE	Linear low density polyethylene

LIST OF TABLES

LIST OF FIGURES

1. Introduction

Thermoplastic polymer composites is a mature field in which research has focussed on the mechanical behaviour of such materials. The emphasis has been on the use of fillers as reinforcing agents for a polymer matrix. In most cases the polymer formed the matrix material with the reinforcing agent suspended as discrete particles or fibres. The use of such reinforcing fillers can improve the thermal and mechanical properties of polymers. The choice of the particular filler will determine the ultimate properties that can be achieved. Most work was done for systems where the volume fraction of the polymer phase was above 70%. Very little research has been done for the case where the thermoplastic is present as the minor phase, i.e. volume fractions below 50%.

For commercial applications, the cost-performance ratio is an important criterium. Since the polymer is usually the more expensive component, effort is focussed on maximising filler content. However, there is a limit to the amount of filler that can be incorporated while still retaining thermoplastic processability. This limit depends on particle form, shape and size distribution. For monodisperse spherical particles the theoretical volume fraction limit is approximately 62%.

In some applications, where the polymer simply acts as a binder, the thermoplastic processability of the composite is of secondary importance. Such materials can be processed using techniques such as compression moulding to produce products in final form. Potential large scale applications include ceiling- and wall sheets.

Mica is a sheet-like mineral, commercially available in the form of muscovite or phlogopite. Muscovite is used in thermoplastic polypropylene compounds where its use leads to significant improvement in the heat deflection temperature. Phlogopite is seldom used as a reinforcing filler

owing to its dark brown colour. However, very large volumes of relatively pure phlogopite are produced as a mining by-product by Foskor in Phalaborwa. The interest in phlogopite, for the purposes of this study, is twofold. Firstly it is available in abundance and at a very low cost. Secondly it has outstanding properties with respect to fire and chemical resistance, that make it eminently suitable for the building industry, especially for low-cost housing.

In principle any thermoplastic can be used as binder for such composites. However, considering the processability and cost of the composite, linear low density polyethylene (LLDPE) was selected for its relatively low cost, excellent processability and a balance between toughness and rigidity. It was therefore decided to use this polymer, with appropriate modifications, as binder.

The present study considered three different aspects of compression moulded sheets:

- the optimisation of the formulation, i.e the selection of the binder, binder content and particle size of the phlogopite filler;
- the optimisation of the processing conditions, i.e the effect of temperature, pressure, compaction time and composite thickness;
- modelling of the mechanical properties, specifically the prediction of Young's modulus of such composite sheets in the plane of reinforcement orientation.

The study is, however, limited to small scale production under a controlled environment. The scaling up to larger composite material dimensions was not investigated.

2. MICA

2.1 Introduction

Mica is a hydrous aluminium-silicate with a highly laminated sheet-like structure. The most common types are muscovite, biotite and phlogopite. [1,2] The three types differ with respect to the proportion of iron, magnesium and aluminium contained within their crystal structures.[1] The most important industrial varieties are aluminium rich muscovite (white mica) and magnesium rich phlogopite (amber mica). Important physical properties of muscovite and phlogopite are listed in Table A6.

Commercially mica is available in the form of sheets and powder. Sheet mica is the most valuable and is derived from large crystals that can be cut, stamped or punched for electrical applications.[1,2] Mica products in sheet form can also be made by a papermaking like process or by binding overlapping small flakes with a suitable cement or a borosilicate glass. [1] Powder forms produced by dry and wet grinding techniques differ in their properties and find a wider application. The main properties that make mica a valuable mineral in industrial applications are listed in Table 1.

2.2 Applications of mica

The primary uses of mica in the 19th century were stove-windows, shades for open flame lights and furnace peep-hole covers. Mica has become a material of paramount importance for its various industrial uses in the modern era. Commercially, mica is processed in a number of forms, namely, natural sheet mica, micanite or built-up mica and mica paper or reconstituted mica. These forms are used primarily in the domestic

electronics and electrical industries. Ground mica, another important form of mica is used in construction, plastic, rubber, paints, printing and other industries. [2,4]

Table 1: Attractive properties of Mica [1,2,3]

Property	Advantages
Chemical	Chemically inert to acids, alkalis and organic solvents and oils even at high temperatures.
Mechanical	Good shape stability. High elasticity. High shear and compressive strength. Perfect cleavability, incompressible.
Electrical	High dielectric strength, high surface and volume resistivity, ability to resist sparking and corona effects
Thermal	High thermal stability, low thermal conductivity, non-flammable and infusible
Optical	Translucent in thin films, absorbs and is stable to UV.
Other	Moisture resistant

Splitting mica is chiefly used as raw material in the manufacture of built-up mica or micanite products.[4] Coarse ground mica flakes find use in oil well drilling, ornamental displays, as automotive components, refractory bricks and surface coating. It provides fire resistance, sound absorption and mechanical strength. [4]

In 1995 the polymer industry, in North America, consumed 134000 tons of mica (muscovite and phlogopite). Of the total mica consumption, 25% was used in the plastic industry and 20% in the paint industry. Phlogopite, in the plastic and paint industry, accounted for 22% of the total mica market. [5]

2.2.1 Construction

Mica is added at 4 - 20 % to cement and plaster mixtures for application in wall sheets, asphalt felts, roof shingles and insulating materials. Advantages imparted by mica include increased resistance to sulphide and chloride corrosion; decrease in the apparent viscosity allowing lower water to cement ratios; increased toughness and shape stability and improved tensile and bending strengths. [1]

The main construction application in the USA is as wallboard joint cement where it is used to fill the gaps between individual boards. Incorporation of dry ground mica improves flow properties, builds body, reduces shrinkage and cracking and provides a smooth, non-absorbent surface. The thin platelets also provide surfaces for the cement to bond onto. These same properties make mica valuable as a filler for all types of sealants for porous surfaces such as wall board masonry, concrete slabs and as a crack filler. [1]

Mica is also used in acoustic and thermal insulation applications including fire resistant gypsum boards. [1]

2.2.2 Coatings

Up to 20 - 40% micronised mica can be added to specialist paint and coating formulations. The reason for use varies from simply being a pigment extender, to mechanically reinforcing the paint, reducing sagging and running, improving anti-corrosive properties, improving resistance to UV degradation and imparting decorative effects such as texturing and sheen. Mica can also be used to substitute up to 25% of the aluminium in silver paints to reduce cost. [1]

2.2.3 Fillers in Plastics

Mica is a relatively low cost filler that improves thermal and dimensional stability, compression and bending modulus, resistance to UV [5] and dielectric properties. It can also improve the notched impact strength of some polymers. It is used in polypropylene to increase the heat deflection temperature (HDT).[5] In high-density polyethylene films the addition of mica increases tearability. It is also used in rotomoulded tanks to reduce permeability to chemicals and vapours. [1]

2.2.4 Electrical and electronic

These markets use mica mostly in sheet form although built-up mica is now being used as a substitute. Applications include electrical heating appliances as well as electric and lighting controls. [1] Mica is known to have excellent dielectric properties. However, in single sheet form it is extremely rigid and is only suitable as support for conductive or resistive wiring [6]. It is also used in the manufacture of fire resistant cables where the mica is applied as a tape to form a fire barrier.

2.2.5 Welding electrodes

Mica is essential in the manufacture of quality welding electrodes. It creates an insulating surface on metal wires, helps to produce meltable slags and prevents welds from cracking. There is currently no substitute for mica in this application. [1]

3. POLYMERIC COMPOSITES

Fillers are used as volume extenders or to improve physical and mechanical properties of polymers. Fillers used to increase the bulk volume of a polymer are known as extenders. Functional fillers, on the other hand, improve mechanical or physical properties. They can be subdivided into functional additives and reinforcements. [7] The former improve physical properties such as thermal or electrical conductivity. Reinforcements improve mechanical properties such as heat deflection temperature, stiffness, impact strength and breaking strength. [7,8]

Mica can act as either a functional filler or as reinforcement. Mica is chemically inert, except to concentrated sulphuric acid and hydrofluoric acid. Muscovite is transparent to UV radiation while phlogopite is opaque.[5] Therefore, phlogopite can contribute to the UV stabilization of the polymer to which it is added. Mica can withstand high temperatures and will not support combustion. [5] The addition of mica can also improve the fire resistance of polymer products such as wall boards, that shield the flammable material from the flame. [10] Mica can also delay, to some extent, the onset of thermal degradation of thermoplastics to which it is added.[9] The thermal resistance of a filler-polymer composite is due to a combination of good structural integrity, low thermal conductivity of the filler and endothermic decomposition pathways. These effects slow down heat transmission through the composite. [11]

Usually it is not possible to optimise the reinforcement properties, e.g. impact strength and stiffness independently. These properties are not affected in the same manner; some may improve while others actually decrease [8], but this depends on the type of filler and polymer used. Therefore it is important to clearly define what is meant by reinforcement.

3.1 Reinforced polymers

3.1.1 Mechanism of reinforcement

The reinforcing action of functional fillers can be attributed to several factors: [7]

- the large difference in stiffness and strength between filler and matrix
- the volume that the filler particles take up
- the formation of chemical bonds between filler and matrix
- slipping that may occur at the filler matrix interface.

Fillers, unlike typical polymers, are characterized by a very high degree of dimensional stability. This implies that the volume that the filler particles occupy is not accessible to the polymer chains. Furthermore, the polymer chains tend to adsorb on the filler surfaces. The segments may attach to the surface through primary and secondary valence bonds. This restricts the motion of the polymer chain molecules as the number of available chain conformations is reduced. Thus polymer segments adjacent to the surface of the filler particles are immobilized. This also leads to the formation of a zone directly at the filler surface that is more ordered than the rest of the polymer matrix. Therefore the filler particles act as physical cross-links preventing chain slippage thus stiffening the material as a whole. [7]

Important parameters that influence the mechanical behaviour of reinforced polymers are:

- the shape and orientation of the reinforcing agent [12]
- particle size [13] and its distribution [14]
- the filler concentration [13]
- the level of interfacial adhesion [13]

Shape of the reinforcing agent

The five common filler shapes are summarized in Table 2. [8] They are grouped into three categories according to their dimensionality, i.e. one dimensional (e.g. fibres), two dimensional (e.g. flakes) and three dimensional (e.g. spheres). [15]

When optimum reinforcement with respect to moduli is desired, the chain confinement effect of fillers implies that the area-to-volume ratio (A/V) should be maximized. For fixed particle volume, the A/V ratio for a sphere is fixed. However, for fibres and flakes it can still be changed by manipulating the aspect ratio.[8] The implication is that both the size and shape determine the surface area of the filler particles. [8,15]

Table 2: Summary of five common filler shapes. [8]

	Group				
	3-D			2-D	1-D
Particle class	Sphere	Cube	Block	Flake	Fiber
Description	Spheroidal	Cubic Prismatic	Tabular Prismatic	Platy Flaky	Fiber
Examples	Glass- spheres Micro-spheres	Calcite Feldspar	Calcite Silica Barite Nephelite	Kaolin Mica Talk Graphite	Wollastonite Tremolite Wood flour
Typical A/V*	High	High	High	Low	Medium

* Area to volume ratio

Mechanical properties, including shrinkage, in materials reinforced with spherical particles are almost isotropic. Reinforcement with spheres may lead to increased compressive strength, as well as improved flexural modulus, but it tends to decrease impact strength. [7]

In fiber reinforced polymers the fibre orientation is very important as it allows anisotropic reinforcement of the polymer. However, random fibre orientation leads to near isotropic mechanical properties. Fibre reinforcement leads to an increase in tensile and flexural strength in the orientation direction. Plane isotropy is also possible but it is more common to use fibres for unidirectional reinforcement. The fibre aspect ratio (length-to-diameter ratio) also affects the reinforcement action. With increasing fibre length more surface area is available for interaction between the polymer chains and the reinforcement. Long fibres allow better stress transfer between matrix and reinforcement.

Unfortunately, anisotropic fibre orientation also leads to anisotropic shrinkage of parts during moulding. The differentials in shrinkage may lead to warping of moulded parts. [7]

The effect of plate-like reinforcements is intermediate between that of spheres and fibres. The flaky shape of the fillers leads to modification of the polymer properties in two directions. Once again the aspect ratio of the flake particles plays a significant role; higher aspect ratios leads to better reinforcement owing to the higher surface area generated. The increased surface area leads to stronger interaction between the polymer chains and the surface of individual filler particles. Reinforcement with flakes leads to an increase in tensile and flexural strength [7], but compared to fibres the reinforcement effect is less. However, overall shrinkage is reduced and part warping is less likely. Furthermore, the presence of resin-rich regions, voids or flake imperfections, as well as poor adhesion and inhomogeneous sites, will lower the strength of a composite. [16]

Two dimensional orientation with platelet fillers leads to a lamellar micro structure. Owing to the increased tortuosity of the diffusion path, such materials exhibit reduced gas and vapour permeability. Important factors that control barrier properties are platelet size, aspect ratio, concentration, size distribution, orientation and interfacial adhesion. [12] Lamellar morphologies may be induced through flow orientation, in processes such as drawing or calendering. [12] Apart from flow induced orientation, self orientation comes into play at high filler volume fractions.

Commercially available mica flakes tend to be highly irregular with respect to their diameter and thickness. When mica is used at low dosage levels, the alignment is random if not specifically orientated by external means.

Järvelä and Järvelä [8] found that combinations of various different filler shapes can provide improved reinforcement. For example, the combination of fibres and platelets showed strong synergy with respect to the flexural strength in polypropylene. [8]

Particle size and distribution

In general particles that are too large may act as points of discontinuity in the composite and may therefore have an adverse effect on mechanical properties. The ideal filler thus has a high aspect ratio and a size distribution with a particle size cut-off at the higher end.

Busigin et al. [17] found that the modulus of mica-filled polypropylene composites is dependent on the flake aspect ratio, whereas the strength is influenced more by the size, i.e. the flake diameter. This implies that in order to maximise both modulus and strength, smaller particles with a large aspect ratio are to be preferred. [17]

Filler concentration

At low filler contents (<10% by mass) reinforcements have little effect on material properties. [8] Mechanical property enhancement is most dramatic at the higher levels of filler content. [18] In general, adding fillers reduces impact strength, but improves rigidity and breaking strength. Thermoplastic polymers are rarely filled beyond 30% by volume. Higher loadings are difficult to process and lead to a loss of mechanical properties. Ultimate properties, such as tensile strength, are very sensitive to complete filler wet-out by the polymer. This necessitates the use of coupling agents at high filler loadings.

Adhesion

It is generally acknowledged that different mechanisms of adhesion work, alone or sometimes together in a particular system. Presently four mechanisms are generally recognized: mechanical interlocking, interdiffusion, electrostatic attraction and chemical interactions. These forces work at different scales of distance between the materials: from the atomic scale for chemical bonds to an undetermined scale in the case of mechanical interlocking. [41]

Situations where mechanical interlocking may be relevant are those when the solid material are very porous and when the adhesive solidifies it forms a sort of anchoring. A similar case is that of the presence of protrusions, around which the adhesive can solidify. The question, however, remains whether mechanical interlocking is a mechanism on it own, or if it simply increases the efficiency of other mechanisms due to the increased surface area.

Interdiffusion only has relevance between two compatible polymers where chains of the one moiety diffuse, at least partially, into the other. With regards to electrostatic attraction it's contribution is usually very small and only occurs when both surfaces has a nett charge. [41]

Chemical interactions between two bodies embrace a variety of forces, such as non-polar dispersion forces, dipole-dipole interactions, dipole- induced dipole interactions and the formation of true chemical bonds.

The examination of the various theories made on the basis of adhesion, and specifically referred to polymers, has shown that only those based on chemical interactions have a general character and a wide application. Since various types of interactions and bonds can be established, the occurrence of them strictly depends on the chemical nature of the materials under consideration. [41]

The performance of composites is strongly influenced by the nature of the interface between the polymer and the filler. Consequently surface modification plays a major role in the manufacturing of composites. [8,19,20,21,22] The effectiveness of the reinforcing agent depends on the aspect ratio as well as the effectiveness of the adhesion between the polymer and the filler. [20,23] If there is no adhesion, the filler particles simply represent flaws that may actually decrease the load bearing ability of the polymer. Adequate adhesion is a prerequisite for stress transfer between reinforcing filler particles and the matrix. [24]

The filler particle surface is inert and therefore chemical bonding between the polymer chains and filler particles surface usually does not occur. Several strategies are available for improving the interaction between filler and polymer. These include the use of coupling agents, surface active agents, organic surface coatings on the filler and modifying the polarity of the polymer.

Coupling agents may provide suitable bonding between the filler and polymer. They attach to the filler particle surfaces either chemically or through physical bonds such as van der Waals forces. The opposite end of the coupling agent molecule is able to chemically bond to the polymer chains. Thus coupling agents chemically bind the polymer chains to the filler particles. Good coupling agents will improve the following properties of the composite: [19]

- the wettability of the filler surface by the polymer.
- the shock absorbing and stress releasing properties of the interface
- the mechanical strength of interfacial layer.

Many different coupling agents are available. The final physical properties of the composite depend on the type and concentration of the coupling agent as well as the method and conditions used to incorporate it. [18] In addition to improving adhesion between the filler and the matrix, coupling agents also modify the rheological properties. A reduction in melt viscosity aids filler de-agglomerisation and can also improve flake alignment. [18]

Conventional coupling agents include silanes, zirconates and titanates. [19] Silanes have been used as surface modifiers for mica. [8,17] Their use improves the wettability and dispersion of the filler in the matrix and eliminates voids due to uneven packing. [22]

Newman and Meyer [18] state that a ductile matrix with adequate interaction between phases is required for proper stress transmission between polymer and filler and to minimize the effect of defects in morphology. [18] In polymer composites failure may initiate in the bulk polymer, at the polymer/filler interface or within filler particle agglomerates. [16] Depending on the strength of the interfacial bonding two failure modes are possible for mica filled composites: flake fracture and flake pull-out. Flake pull-out and separation prevent full utilization of the filler's strength. [18]

Surface active agents can also be used to improve interfacial adhesion as well as the dispersion of fillers in a matrix. For example, stearic acid is used with basic fillers such as calcium carbonate. [16]

Surface coating techniques can also be used to advantage. Inubushi et al. [40] reported improved adhesion in mica filled ABS when treated with an aminimide cured epoxy resin, where it improved the flexural strength of the composite.

Finally, the affinity of non- polar polymers for the ionic fillers can be improved by incorporating polar groups on the chain. Grafting a polar monomer onto a non-polar polymer improves its adhesion to fillers. For example LLDPE can be modified by graft copolymerisation with polar monomers, e.g. acrylic acid or maleic anhydride. Typically the grafting reaction is peroxide initiated. At low dosages of monomer and initiator the tendency for cross linking is reduced, but homopolymerisation may still occur as a side reaction. [16] In the absence of adhesion only mechanical interlocking exists between the filler and the polymer. [21]

An alternative to grafting is to modify the polymer by irradiation with an electron beam or with gamma rays. This process introduces polar groups onto the polymer chains due to controlled oxidation thereby increasing adhesion ability. [25]

SEM analysis of a fractured surfaces is a powerful tool to qualitatively assess the interfacial bonding in a composite. [39] SEM photos of an epoxy / mica composite revealed smooth filler surfaces when interfacial adhesion was poor (adhesive failure). In contrast, for strong adhesion, threadlike features were visible due to cohesive failure of the polymer. [24]

3.2 Particulate composites with a polymer as binder

Reinforced polymer systems generally contain less than 50% (by mass) filler. Particulate composite systems represent the other side of the spectrum comprising much higher contents of granular fillers. [14] Here the polymer simply acts as a binder for the fillers.

3.2.1 General concepts

There are two theories that are used to describe particulate composites: the filler theory and the mastic theory. [14] The filler theory states that the composite achieves optimal properties when the particle size distribution allows maximal packing efficiency. According to the mastic theory the polymer produces a coating on each filler particle with optimal thickness. This film provides the bonding contact between the particles that leads to a stable and strong composite structure. [14]

3.2.2 Factors influencing composite properties

As in reinforced polymers the mechanical properties of particulate composites are determined by the filler to binder ratio, filler size and distribution and the degree of wetting and adhesion that is achieved between the filler and the polymer. [14]

However, processing factors also influence the properties of a composite. In thermoplastic compression moulding, these include tool design, tool temperature, preheat temperature, moulding pressure and time at pressure. Preheat temperature was found to contribute most to the final properties of a commingled glass and polypropylene composite. High preheat temperatures result in reduced polymer viscosities. This aids the impregnation of the polymer into the glass fibre bundles and allows for compaction to occur. [26] While high pressures are needed to reduce void content, pressure was a less important parameter than the preheat temperature. [26]

Sidess et al. [14] have shown that more polymer is needed to wet smaller particles than larger particles. Thus the smaller particles play an important role in determining the optimal matrix content for enhanced mechanical properties. To obtain a stiffer material dense packing is required while for compressive strength the matrix should have a measure of ductility. The results of Sidess et al. [14] showed that all the mechanical properties attain maximum values at the same particle size distribution. However, for other formulation variables this is not the case, e.g. filler to binder ratio.

4. YOUNG'S MODULUS

In practice both the strength and stiffness of particulate composites are important. Ahmed and Jones presented an extensive review of the available theories for predicting these properties. [24] The theory for the strength of particulate composites is less developed than that for moduli. This is because it involves many more factors that need to be considered, i.e. the complex interplay between the properties of the reinforcement, the polymer and the interfacial layer.[24] Variables that are important include the shape, size and distribution of filler particles and the strength of the interfacial bond between filler and matrix. The fact that the reinforcements are discontinuous complicates the analysis. The reinforcing agents may have a non-uniform size and may even be non-uniformly distributed in the matrix. [27]

Fibrous reinforcements allow properties to be maximized in the direction parallel to the fibre orientation. [27] Planar reinforcements allow mechanical properties to be developed in the plane of the reinforcement. Such planar reinforcements include: flakes, ribbons and continuous films. [27] Mica, the filler of interest in this study, approaches a flake structure. The focus of this chapter is on methods to predict the modulus of planar flake reinforced composites. A more detailed review is given by Ahmed and Jones. [27]

4.1 The Young's modulus for lamellar composites

The available models for predicting the Young's modulus vary from empirical to highly theoretical. One of the simplest models idealise the composite as alternating layers of high modulus reinforcement and a more compliant matrix. The elastic properties of these laminated composites depend on their orientation relative to the applied stress as shown in Figure 1. The assumption is made that the layers are strongly bonded and this implies that the volume fraction, rather than the thickness of the individual layers determines the mechanical properties. The effective moduli when the layers are in parallel or in series

yield the Voigt and Reuss average moduli respectively. [28] Maximum stiffness is obtained when the stress is applied parallel with the layers. The assumption is that the strain will be the same in all the composite layers, i.e. the isostrain condition applies. The effective Young's modulus is given by Equation 1A.

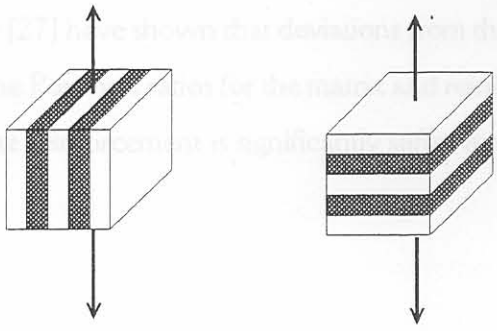

A: Isostrain B: Isostress

Figure 1: Mixing rule conditions for layered composites

When the layers are orientated transverse to the applied stress, the effective modulus is much lower. (Figure 1B) In this case each layer is subjected to the same force. As it is assumed that the area remains constant through the stack, the stress is also the same in each layer, i.e. the isostress condition applies. The effective modulus for this case is given by Equation 1B.

$$E_C = E_m V_m + E_p(1 - V_m) \quad \ldots\ldots\ldots\ldots A$$

$$\frac{1}{E_C} = \frac{V_m}{E_m} + \frac{(1 - V_m)}{E_p} \quad \ldots\ldots\ldots\ldots\ldots\ldots B$$

Equation 1: The classical rule of mixtures

By analogy for these theoretically correct models, these equations are also used in the form of mixing rules for more general applications. In summary, the classical mixing rules are then:

- isostrain, where the force acting on the composite is equal to the sum of the forces acting on each of the elements.
- isostress, where the total strain is equal to the sum of the strains in each element. [24,29]

Padawer and Beecher [27] have shown that deviations from the isostress model do occur due to differences in the Poisson's ratios for the matrix and reinforcement. However, this effect is small when the reinforcement is significantly stiffer than the matrix. [27]

4.2 Empirical modifications to the classical mixing rules

Both forms of the mixing rule are applicable to unidirectional long fibre reinforced composites. [24] For composites in general, the isostrain and isostress mixing rules provide upper and lower bounds of the actual behaviour. It is therefore of interest to consider modelling the modulus in terms of appropriate combinations of the mixing rules as in the Hirsch and Counto models. They are based on the geometric models for the composites shown in Figure 2. The Hirsch model (Equation 2A) constitutes a linear combination of the two mixing rules whereas the Counto model (Equation 2B) is more complicated. Both are based on the assumption of perfect adhesion between the two phases.

$$E_c = y(E_p v_p + E_m v_m) + (1-y)\frac{E_p E_m}{E_p v_m + E_m v_p} \tag{2A}$$

$$\frac{1}{E_C} = \frac{1-v_p^{1/2}}{E_m} + \frac{1}{(1-v_p^{1/2})/v_p^{1/2}E_m + E_p} \tag{2B}$$

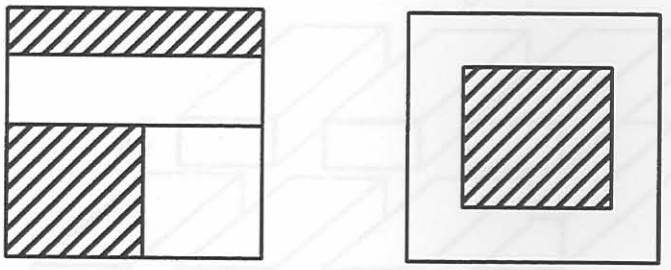

A: Hirsch B: Counto

Figure 2: Schematic representation of the Hirsch and Counto models. [24]

Jacquet et al. have further modified the rule of mixture to account for isolated particulate inclusions, e.g. micro spheres. [29] In essence their model is based on a three-dimensional array of Counto repeat units. Figure 3 shows how the composite is divided into columns

to which the classical rules of mixture are applied to calculate the overall modulus. The result is a parameter free model.

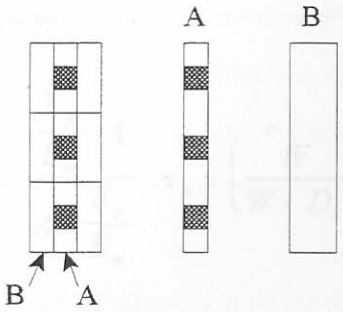

Figure 3: The Jacquet et al. model [29]

$$E = \frac{\alpha^2 E_m E_p}{\alpha E_p + (1-\alpha) E_m} + (1-\alpha^2) E_m \qquad (3)$$

$$\alpha = \sqrt[3]{V_m}$$

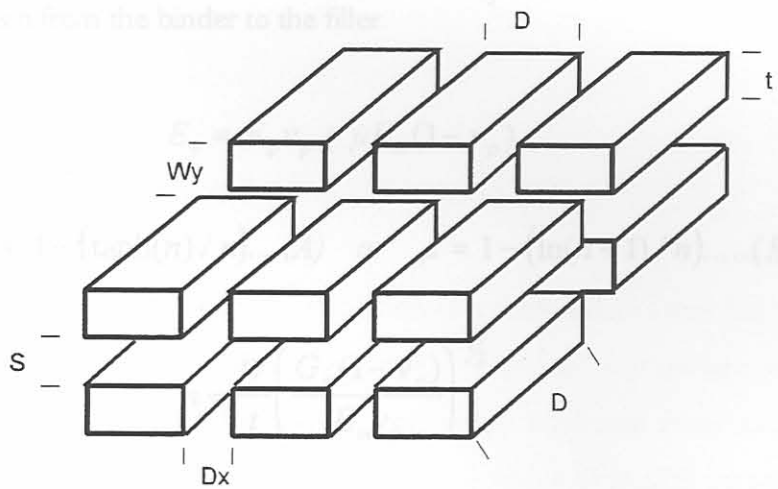

Figure 4: The Halpin and Tsai model [30] for regular platelet or ribbon reinforcement

Halpin and Tsai [30] derived a model for the case of unidirectional plane-parallel ribbon or platelet reinforced composites (Equation 4). E_c is the composite modulus in the plane of orientation (See Figure 4 for definition of symbols). [30] This model reduces to the isostrain mixing rule when L→ ∞.

$$E_c = E_m \frac{1 + ABv_p}{1 - Bv_p} \quad B = \frac{\frac{E_p}{E_m} - 1}{A + \frac{E_p}{E_m}} \quad v_p = \left(\frac{W}{W + D_x}\right)\left(\frac{D}{D + D_x}\right)\left(\frac{t}{t + S}\right) \qquad (4)$$

$$A = 2\left(\frac{W}{t}\right)$$

To calculate the transverse in-plane-of-orientation modulus , L/t can be replaced by W/t. To calculate the transverse out-of-plane modulus, the inverse mixing rule can be used.

The models developed by Padawer and Beecher [27] (Equation5A) and Lusis et al. [24] (Equation 5B) assume a stress transfer mechanism between the polymer and the filler. However, only the model by Lusis et al. [27] accounts for platelet interactions at high platelet concentrations. [18,30] It is also assumed that stress is transferred via a shearing mechanism from the binder to the filler.

$$E_c = E_p v_p + \mu E_m (1 - v_p)$$

$$\mu = 1 - \left(\tanh(n)/n\right)....(A) \quad or \quad \mu = 1 - \left(\ln(n+1)/n\right).....(B) \qquad (5)$$

$$n = \frac{W}{t}\left(\frac{G_p(1 - v_p)}{E_m v_p}\right)^{1/2}$$

The Kerner and Lewis [23] model (Equation 6) takes into account that the mechanical behaviour of composites depends on the degree of interfacial adhesion between the

phases, the maximum packing fraction of the filler (ϕ_m) and the Poïsson's ratio of the polymer (ν_{ps}). The model assumes the following:

- initially all filler particles are well bonded to the matrix. ($\phi_d=0$)
- as the material is strained the filler becomes progressively debonded from the matrix (ϕ_d = debonded filler volume fraction)
- the completely debonded composite behaves similar to a foamed matrix ($\phi_d = \nu_p$)

The incorporation of a void faction due to the debonding process, lowers the effective modulus of the composite.

$$E_c = E_p E_1 E_2$$

$$E_1 = \frac{1 + A_1 B_1 (v_p - \phi_d)}{1 - B_1 \psi (v_p - \phi_d)} \qquad E_2 = \frac{1 - \phi_d}{1 - B_2 \psi \phi_d} \qquad A_1 = \frac{(7 - 5\nu_{ps})}{(8 - 10\nu_{ps})} \tag{6}$$

$$B_2 = -\frac{1}{A_1} \qquad \psi = 1 + \frac{v_p (1 - \phi_m)}{\phi_m^2}$$

4.3 Limitations of existing theoretical models

Most models described in literature assume that the polymer forms the continuous phase with the filler suspended in it. Practically composites may deviate from the idealized models if the filler particles are not completely separated from each other and the reinforcement element will therefore be an aggregate of smaller particles. The applied stress will therefore not be distributed evenly between the particles and the aggregates and the assumption of either isotress or isostrain will not be valid.

Furthermore, the most general assumptions are:

- the reinforcement and polymer are linear elastic materials, with uniform moduli
- the flakes have uniform width and thickness
- the flakes are uniformly spaced and aligned in a plane-parallel fashion
- the polymer adheres perfectly to the reinforcement.

In Chapter 3 it was shown that the mechanical properties of a composite depend on many factors including:

- the volume fraction filler
- the adhesion between the phases
- particle size and distribution (and therefore aspect ratio)
- shape and orientation of the filler
- the voidage in the composite.

Any model that predicts the mechanical properties of a composite should therefore account for these variables. However, most theoretical models predict that the mechanical properties of the composite only depends on the volume fraction of the filler. This represents a serious limitation for all these models.

The effect of particle shape, orientation and size distribution will show up in the maximum possible packing of a filler. Polydispersed particle mixtures can pack more densely since smaller particles can fill the voids between larger particles. [27] Odd shaped particles will also pack more loosely than highly regular particles such as spheres. One model that does recognise this phenomenon is the Kerner and Lewis equation. [23] Despite other limitations of this model [27] this is one of the few models that does consider the influence of other factors on the mechanical properties of the composite.

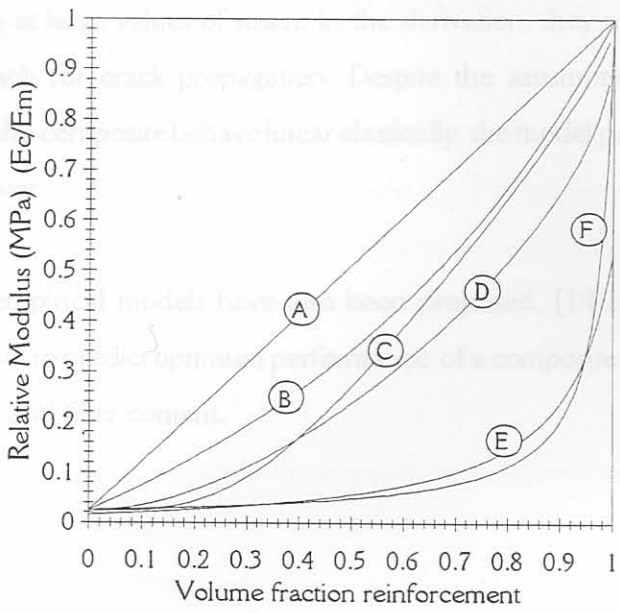

Figure 5: The predicted variations of the tensile modulus of a composites: A: Isostrain (1A), B: Jacquet el al. (4) , C: Padawer and Beecher (5A), D: Lusis et al. (5B), E: Kerner and Lewis (6), F: Isostress (1B). Quantities in brackets indicate the equation numbers in the main text.

A good model will provide accurate prediction over the whole concentration spectrum. Most of the models discussed in the previous section are based on various modifications to the mixing rule. Figure 5 shows the predicted effect of volume fraction on the relative modulus. All these models suffer the same drawback. They all predict that the composite modulus will approach the filler modulus when its volume fraction approaches one. Considering that the filler is present in the form of discrete particles, this is clearly incorrect. A bed of loose filler particles is expected to have no tensile properties unless the filler particles are bound together. This obviously implies the presence of a binder.

Any model used to describe the mechanical behaviour of particulate composites should therefore be able to predict a decrease in mechanical properties, approaching zero, as the amount of binder present approaches zero volume fraction. Additional effects such as voidage should also be considered. The presence of voids will lower the modulus of the composite because they cannot carry any load.

Anderson [13] derived a model that takes into account the debonding process between filler and matrix at large values of strain. In the derivation, they used the Griffith energy balance approach for crack propagation. Despite the assumption that the individual components of the composite behave linear elastically, the model predicts highly nonlinear stress-strain curves.

Various other empirical models have also been proposed. [14,16,24] Some even use experimental data to predict optimum performance of a composite with respect to particle size distribution and filler content.

5. MATERIALS AND METHODS

The objective of the wider study, of which this work forms part, was to investigate the feasibility of phlogopite-LLDPE composites for building applications. The prime objective was to reduce cost to a minimum. Amongst other factors this also requires minimisation of the expensive binder in the composite. The current study reports on the measurement and prediction of the Young's modulus of such composites. The experimental investigation was conducted in four parts:

- Initial scoping experiments were conducted to determine relevant ranges of the independent variables.
- With knowledge of these preliminary results, a statistical experiment was designed, using the Taguchi approach, to determine the relative contribution of the composition variables.
- Next, a similar approach was followed to evaluate the effect of processing.
- Finally, based on these results a new predictive model for the composite modulus was developed. Additional experiments were also performed in order to verify its validity.

To fully characterise the mechanical properties of composites it is necessary to conduct many different measurements. A composite's tensile properties depend on its micro-structure, interfacial load transfer between two phases, and structural factors such as form, size distribution, aggregation and orientation of the filler. [16] It is important to note that these give complementary information on the material properties. Modulus data, in contrast to impact strength, is not very sensitive to structural defects and the degree of adhesion between the filler and matrix. This is because it is evaluated at low deformations and low strain rates. Tensile strength and elongation-at-break are large scale deformation properties and are more sensitive to structural defects. Filler surface treatment, in general, has a greater effect on the latter properties than on modulus. On the other hand, for the case of laminar composites, flexural tests should also be performed to highlight any interlaminar effects. [26]

5.1 Experimental procedure

Figure 6 outlines the procedure followed to produce the phlogopite-based composite sheets: (Details are provided in Appendix 3)

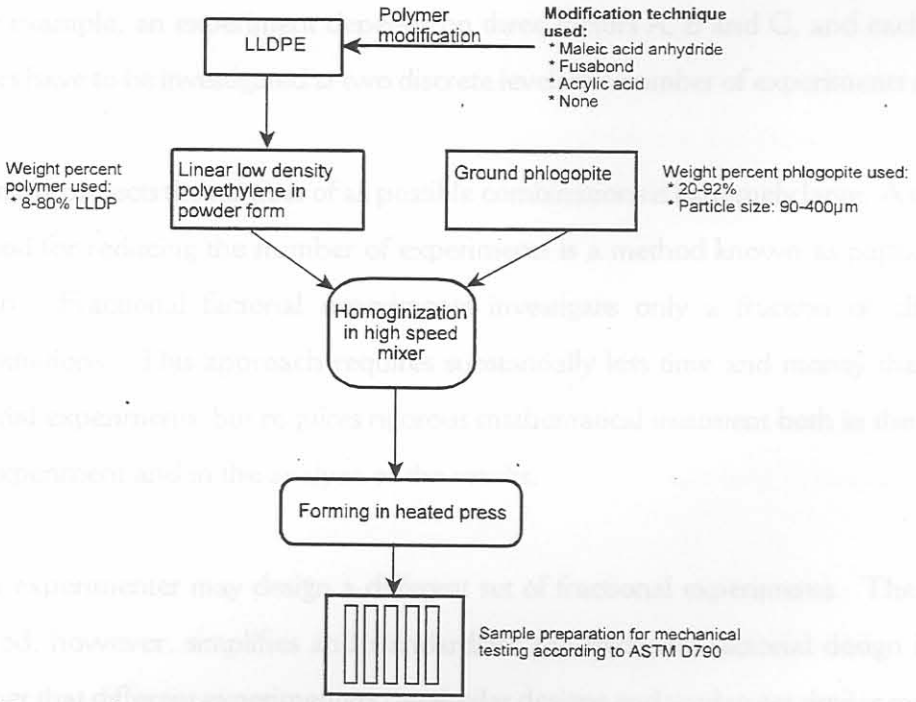

Figure 6: General outline of the experimental procedure followed

Five test pieces were cut from each sheet to obtain the necessary test pieces for a flexural three point bending tests (for bending modulus and yield strength), tensile tests and Izod impact tests. All the tests were performed according to ASTM standards [31,32] at 50% humidity and 25°C.

The Taguchi experimental design technique

The technique used for defining and investigating all possible conditions in an experiment involving multiple factors is known as factorial design. This method enables an experimenter to determine all possible combinations of experimental variables and to identify the best combination for a required result.

If for example, an experiment depends on three factors A, B and C, and each of these factors have to be investigated at two discrete levels the number of experiments are $2^3=8$.

For many projects the number of all possible combinations is extremely large. A customary method for reducing the number of experiments is a method known as partial factorial design. Fractional factorial experiments investigate only a fraction of all possible combinations. This approach requires substantially less time and money than the full factorial experiments, but requires rigorous mathematical treatment both in the design of the experiment and in the analysis of the results.

Each experimenter may design a different set of fractional experiments. The Taguchi method, however, simplifies and standardizes the fractional factorial design in such a manner that different experimenters use similar designs and tend to get similar results. [35]

Taguchi constructed a special set of orthogonal arrays to design his experiment. A typical orthogonal array is shown in Table 4 and Table 5. This array designated by the symbol L_{16} is used to design experiments involving up to four factors at four levels each. Each row represents a trial condition with factor levels indicated by the numbers in the row. The vertical columns correspond to the factors specified in the experiment.

The standardized orthogonal arrays of the Taguchi method facilitates the experimental design process. To design an experiment the most suitable array has to be selected from several pre-defined arrays available, depending on the number of factors and levels used in the particular experiment.

In the Taguchi method the results are analyzed to achieve on or more of the following objectives [35]:

- to establish the best or optimum condition for a product or process
- to estimate the contribution of each individual factor
- to estimate the response under optimum condition

The optimum condition can be identified by studying the main effects of each of the factors. Referring to Table 4, the main effect of e.g weight percentage polymer at level 3 will be the sum of the result of all the trials containing this factor at level 3. The optimum level for this factor will then be the level with the largest (or smallest, if appropriate) main effect. [35]

The analysis of variance (ANOVA) is the statistical treatment most commonly applied to the results of the experiments to determine the percentage contribution of each factor. By studying the ANOVA results for a given experiment it can then be established which are the critical factors, that need control. [35]

5.2 Scoping experiments

Linear low density polyethylene was used as binder. To promote adhesion of the polymer to the surface of the phlogopite, various pre-modified LLDPE were tried, viz. irradiated LLDPE from Gammatron (Pty) Ltd [33], LLDPE compounded with 10% maleic acid anhydride (MAA), LLDPE compounded with 5% MAA and LLDPE compounded with 10% MAA and 1% chain transfer agent (C1) to inhibit cross linking. All the polymers were used in powder form and each formulation was homogenised in a high speed mixer prior to compression moulding. Phlogopite was supplied by FOSKOR Ltd. in South Africa [34] and was milled in a laboratory pin mill to an average particle size of 400μm.

Table 3: Experimental design for the scoping experiments

		Polymer System				
		Pure LLDPE	Irradiated LLDPE	10% MAA 90% LLDPE	5% MAA 95% LLDPE	10% MAA 1% Additive
		Experiment #				
% polymer	5%	1	5	9	13	17
	10%	2	6	10	14	18
	15%	3	7	11	15	19
	20%	4	8	12	16	20

Table 3 shows the experiments performed using the materials mentioned above. Two sheets of each composition were made using compression moulding. The mould had dimensions of 150mm wide by 200mm long. Sheets were produced that were 3.5mm thick. The sheets were hot pressed at 190°C at a pressure of 10 MPa and each sample was left at this pressure for 15 minutes to allow proper heat transfer and complete wetting of the phlogopite by the polymer.

5.3 Composition

Virgin linear low density polyethylene (LLDPE) and various pre-modified forms were used. Modifications included: irradiated LLDPE from Gammatron [33], Fusabond from Du Pont and LLDPE blended with 220 mmol acrylic acid per 100g LLDPE. [21] All the polymers were used in powder form and each formulation was homogenised in a high speed mixer prior to hot pressing.

Phlogopite was pin milled and classified in a dry sieve shaker to the desired particle size range. Table 4 shows the experiments performed using the materials mentioned above, following the L_{16} Taguchi array [35]. The variables particle size, type of polymer modification and mass percentage polymer were investigated at four levels as indicated in Table 4.

Two composite sheets of each composition were prepared using hot press moulding. The mould had dimensions of 150mm wide by 200mm long. Sheets (3.5mm thick) were produced by compression moulding at 190°C at a pressure of 5 MPa for 7 minutes followed by 10 MPa for 13 minutes.

5.4 Processing conditions

Fusabond (ex Du Pont) at 15% by mass was used as binder. Pin milled phlogopite in the size range 180 to 150 μm was used as filler. Table 5 shows the experiments performed using the materials mentioned above, following the L_{16} Taguchi array [35]. Process temperature, pressing time, moulding pressure and the mass per unit area were investigated at four levels as indicated in Table 5.

Two composite sheets of each composition were prepared using hot press moulding. The mould had dimensions of 150mm wide by 200mm long. The testing procedure was similar to that for the composition experiments.

Table 4: Taguchi experimental array showing the individual experiments with the results obtained.

Level	Polymer type	wt% polymer	particle size
1	PE	8	90
2	γ-PE	14	125
3	Fusa	20	180
4	AA	24	250

PE - Pure LLDPE
γ - Irradiated LLDPE
Fusa - Fusabond
AA - LLDPE blended with 220 mmol acrylic acid per 100g LLDPE

Exp#	Column			Results (MPa)			
	1	2	3	Flexural modulus	Flexural Stress at Yield	Young's modulus	Tensile strength
1	1	1	1	195	3.9	170	0.3
2	1	2	2	1341	9.5	1641	2.3
3	1	3	3	2333	12.6	2001	2.6
4	1	4	4	1725	16.3	924	1.9
5*	2	1	2	0	0	0	0
6	2	2	1	657	6.1	990	0.8
7	2	3	4	1453	10.8	1045	2.6
8	2	4	3	1185	10.9	1311	1.9
9	3	1	3	289	4.9	1619	0.3
10	3	2	4	1892	12.7	1178	1.6
11	3	3	1	1575	14.4	1042	1.8
12	3	4	2	1276	13	1115	2.6
13	4	1	4	140	3.7	1379	0.6
14	4	2	3	1303	7.2	1112	2.6
15	4	3	2	1481	11.3	1084	1.9
16	4	4	1	1334	11.4	900	2.1

* The composite produced in this experiment was too weak for mechanical testing and therefore no results are available for this particular trial.

Table 5: Taguchi experimental array showing the individual experiments with the results obtained.

Level		Temp °C	Time min	Press MPa	*kg/ m^2
	1	150	5	5	5
	2	200	10	6.5	6.7
	3	250	15	8	8.3
	4	300	20	10	10

Exp#	Column				Results (MPa)			
	1	2	3	4	Flexural modulus	Flexural Stress at Yield	Young's modulus	Tensile strength
1	1	1	1	1	1215	12.2	1880	1.8
2	1	2	2	2	1348	13.8	1856	2.1
3	1	3	3	3	1549	15.3	1724	2.1
4	1	4	4	4	3003	19.1	1439	2.7
5	2	1	2	3	1745	15.8	1186	1.9
6	2	2	1	4	1394	15.2	1729	2.5
7	2	3	4	1	2609	22.6	1564	4.0
8	2	4	3	2	2025	17.1	2374	2.8
9	3	1	3	4	2010	16.9	2044	3.8
10	3	2	4	3	2254	18.5	2110	1.5
11	3	3	1	2	904	11.2	1393	2.1
12	3	4	2	1	2269	23.4	1377	4.4
13	4	1	4	2	2327	23.9	1634	2.2
14	4	2	3	1	1909	21.7	1850	4.5
15	4	3	2	4	2424	21.3	1766	1.1
16	4	4	1	3	1525	17.1	2260	2.1

* The mass of material used per m^2 determined the thickness of the sheet.

5.5 Modelling

Table 6 shows the experiments performed:

Table 6: Experiments for model verification

Method†	mass% polymer	Particle size range*
Compression moulding	8-30% in 2% increments	• 125-180 µm • 250-300 µm
Injection moulding	50, 60 and 80%	• 125-180 µm • 250-300 µm

† Based on the planar isotropic nature of the material the Young's modulus of the composite would only slightly be influenced by the method

* Although the particles were sieved, image analysis revealed that the average aspect ratio was constant at about18

Young's modulus

All samples were prepared and tested in the same manner as described before.

Voidage

The voidage of all the samples was calculated after measuring the density of the samples, using Equation 7.

$$\phi = 1 - \frac{\rho_{composite}}{\rho_{theoretical}} \tag{7}$$

The theoretical density can be calculated from the individual phases' densities, based on the mass fraction of each:

$$\frac{1}{\rho_{theoretical}} = \frac{x_p}{\rho_p} + \frac{x_m}{\rho_m} \tag{8}$$

6. RESULTS

The results obtained in the various experimental sections will be discussed separately as outlined in chapter 5.

6.1 Initial scoping experiments

The results of the mechanical property measurements are presented in Figures 7 to 9. Note that the samples that contained 5% LLDPE were too weak for mechanical testing.

6.1.1 Bending modulus

With the exception of the 5% MAA sample, Figure 7 shows that modification of the LLDPE improves the bending modulus. This may be attributed to improved interfacial adhesion and to a lesser extent to an increase in modulus of the matrix.

It is well known that maleic anhydride modified LLDPE provides excellent adhesion to polar surfaces. The significant improvement in bending modulus of 5% and 10% MAA compared to virgin LLDPE probably reflects an interfacial adhesion effect. In contrast the improvement when the irradiated LLDPE is used, probably reflects matrix stiffening due to cross-linking. It is also known that the use of MAA grafted polyethylene also leads to cross-linking. Therefore the 10% MAA data reflects a combination of adhesion improvement and matrix cross-linking. This is confirmed by the 10% MAA plus 1% C1 data set in which cross-linking was largely prevented.

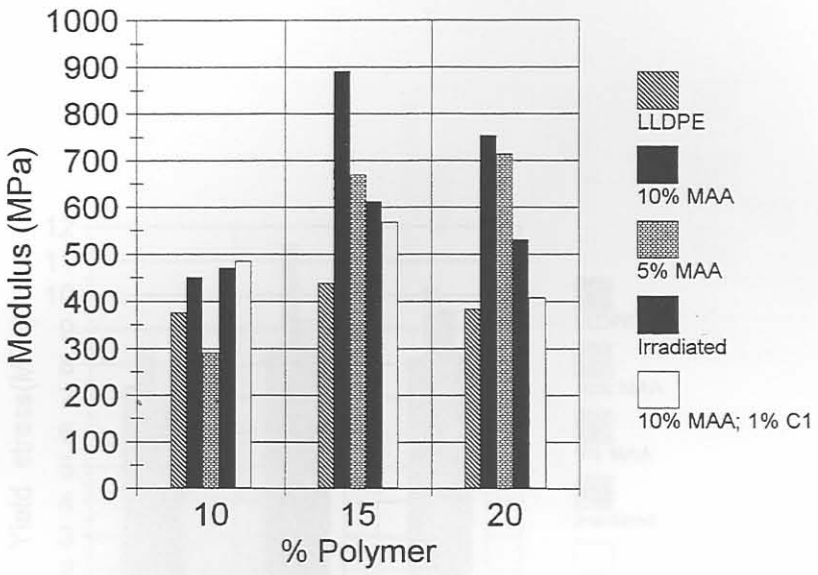

Figure 7: Bending modulus for various modified LLDPE / Phlogopite composites

It is interesting that in all cases the modulus reached a maximum value at about 15% polymer content. This is an unexpected result. It can be rationalised as follows: firstly phlogopite has a much higher modulus than the polymer. At very low concentrations of polymer the phlogopite flakes are not effectively bound and this lowers the effective modulus. At high polymer levels the lower modulus of the polymer becomes significant, again lowering the modulus of the composite.

6.1.2 Yield strength

Figure 8 shows the effect of polymer content and type on the yield stress of the composites. Once again optimum yield stress is obtained at 15% polymer loading. Since it is a large-deformation property, yield stress is expected to be more sensitive to the degree of adhesion between the polymer and the phlogopite than the degree of cross-linking of the matrix. This is confirmed by the fact that there is very little difference in yield stress of the virgin LLDPE and irradiated (cross-linked) samples. Further confirmation for this conclusion is provided for the small differences observed between the cross-linked and

uncross-linked 10% MAA samples. Best performance was achieved using the 10% MAA LLDPE as matrix material.

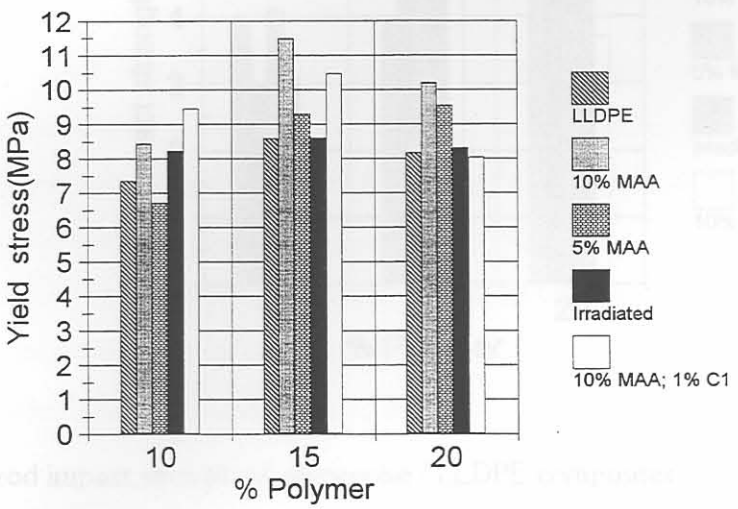

Figure 8 Stress-at-yield for various modified LLDPE / phlogopite composites

6.1.3 Izod Impact strength

Figure 9 shows the impact strength of the various composites tested. From these results it can be seen that the impact strength increases with increasing polymer content, as it is expected. The various modifications to the LLDPE do not influence the impact strength significantly.

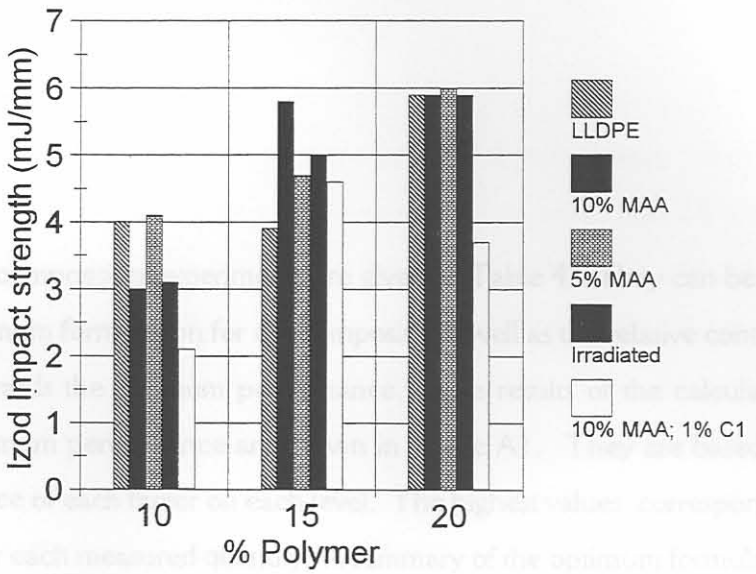

Figure 9: Izod impact strength of phlogopite / LLDPE composites

6.1.4 Appearance

The sheets that were made had an appearance similar to wood composites that are used as dry walling in the building industry. The advantageous properties imparted by the phlogopite, such as low thermal conductivity, good sound proofing and fire resistance will make it ideal for this application.

6.1.5 Conclusions

The initial experiments showed that the bending modulus and yield strength reached optimum values at 15% polymer whereas impact strength increased with polymer content. With respect to the polymer modifications used, it appears that interfacial adhesion is a more important factor than cross-linking. It is assumed that the stiffness of the polymer is increased by the degree of cross- linking. Optimal results were obtained using the 10%

MAA grafted LLDPE. It is assumed that this modification provided improved adhesion and improved matrix stiffness.

6.2 Composition

The results of the composition experiments are given in Table 4. They can be used to determine the optimum formulation for the composite as well as the relative contribution of each factor towards the optimum performance. The results of the calculations to determine the optimum performance are shown in Table A1. They are based on the average performance of each factor on each level. The highest values correspond to the best formulation for each measured quantity. A summary of the optimum formulation for each measured quantity is shown in Table 7.

As shown by Kovačevic et al. [16] and Wakeman et al. [26], tensile measurements provide a better indication of interfacial adhesion than flexural measurements. The present results for tensile stress at break , for the composites bonded with acrylic acid modified LLDPE provided confirmation for this observation .

Table 7: Optimum formulation for each of the mechanical properties

	Polymer type	% Polymer	particle size
Flexural modulus	LLDPE	20%	180-250µm
Flexural stress at yield	Fusabond	24%	180-250µm
Young's modulus	Fusabond	20%	125-180µm
Tensile strength at break	AA	20%	125-180µm

For filled polymeric systems, smaller particles usually have the best reinforcing effect. It is evident from the data, however, that in the case of these composites, larger particles are preferred. It was previously mentioned that more polymer is needed to wet smaller particles. Since the amount of polymer in the system is to be kept as low as possible larger particles are preferred. Analysis of variance revealed that particle size only contributed

significantly in terms of the Young's modulus of the composite. For the other measured variables, the effect of particle size was overshadowed by the large effect of the amount of polymer used.

The results (Table 4) also indicate that more polymer is not always better for the composite properties. Only in the case of flexural stress at yield, was 24% polymer preferred over 20% polymer. The reason for this is most likely due to the role of the interface. At low polymer content there is not enough polymer to wet the phlogopite and effectively bind the composite. At higher polymer concentration, more polymer is present at the interface and the phlogopite may start acting as a weakness in a polymer matrix, which is generally true for polymer systems where the filler is added at quantities more than 60%. From the results of the Taguchi experiments one can see that 20% polymer will generally be the optimum.

6.2.1 Flexural properties

Figure 10 shows the ANOVA results for flexural modulus and flexural stress at yield. A 10% level of significance was used to determine the significance of each factor.

It is interesting to note that for the flexural modulus, particle size does not contribute significantly. When this factor is pooled with the error term it becomes even more clear that the amount of binder is the most important factor relating to the properties of the composite.

It was previously shown [16,26] that the effect of adhesion is more important for ultimate properties than for modulus data. The ANOVA results show that the use of Fusabond improves the yield strength. This effect was not apparent from the modulus data, which suggested virgin LLDPE as the optimum polymer for flexural modulus. In the case of yield strength, the amount of polymer is once again the most important parameter influencing the properties of the composite.

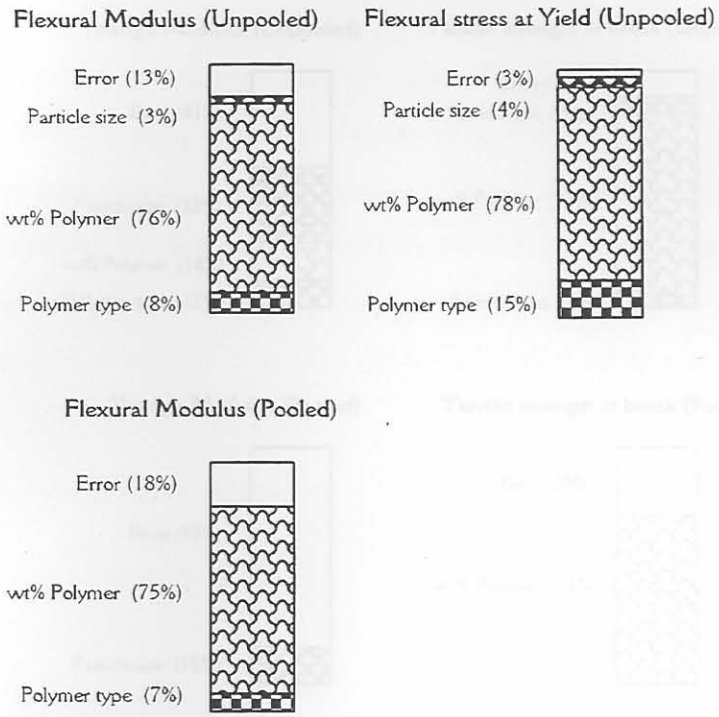

Figure 10: Relative contribution of the composition variables towards the flexural properties (pooled and unpooled)

6.2.2 Tensile properties

Figure 11 shows the ANOVA results for the tensile properties of the composite at a 10% level of significance. It is evident from Figure 11 and Table A2 that none of the measured variables played a significant role in determining the Young's modulus of the composite. This is attributed to the large intrinsic variability in mechanical properties of this complicated system. The low contribution of polymer content factor, to explain the observed variance, can also be attributed to non-linear effects. Furthermore, the Young's modulus is known not to be sensitive to the effects of particle size and efficiency of adhesion. The amount of binder, therefore, also becomes less important in this case, because the stiffening effect of the phlogopite on the polymer is evident even at very low concentrations.

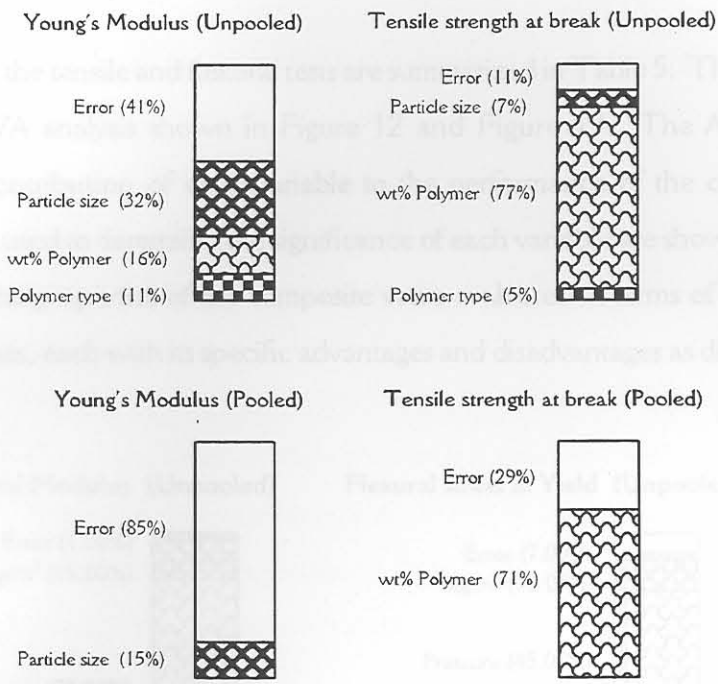

Figure 11: Relative contribution of the composition variables towards the tensile properties (pooled and unpooled)

The tensile strength of the composite is also influenced the most by the amount of polymer used. For a high tensile strength the adhesion between the polymer and the phlogopite needs to be very good. For good adhesion more polymer is needed to wet the surface properly. In other words, using too little polymer, regardless of the particle size, the polymer will not effectively wet the surface thus limiting stress transfer between the polymer and the phlogopite.

6.3 Processing parameters

The data from the tensile and flexural tests are summarized in Table 5. These were used for the ANOVA analysis shown in Figure 12 and Figure 13. The ANOVA results indicate the contribution of each variable to the performance of the composite. The variance ratios used to determine the significance of each variable are shown in Table A4. The mechanical properties of the composite were evaluated in terms of its flexural and tensile properties, each with its specific advantages and disadvantages as discussed earlier.

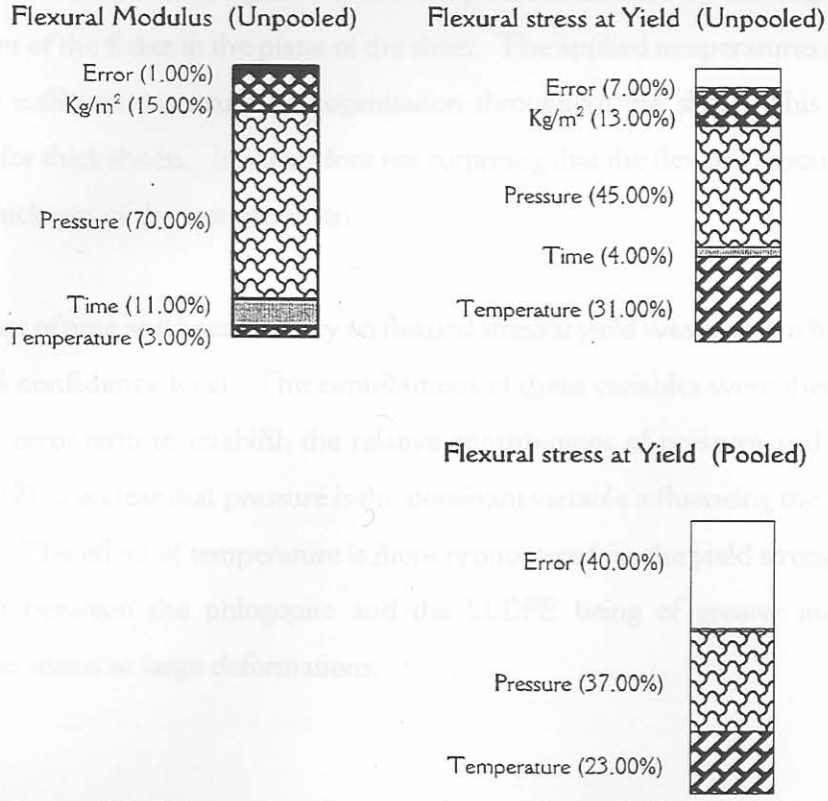

Figure 12: Relative contribution of processing variables towards flexural properties (pooled and unpooled)

6.3.1 Flexural properties

Figure 12 shows the ANOVA results for flexural modulus and flexural stress at yield. A 10% level of significance was used.

It is clear from Figure 12 and Table A4 that all the variables contributed significantly to the flexural modulus. Of the variables investigated, moulding pressure dominated while moulding time and temperature had the smallest effect.

The flexural modulus, or rigidity, of the composite is affected by the degree of parallel alignment of the flakes in the plane of the sheet. The applied temperatures and pressures must be sufficient to ensure homogenisation throughout the sheet. This is difficult to achieve for thick sheets. It is therefore not surprising that the flexural modulus is affected by the thickness of the test specimen.

The effect of time and linear density on flexural stress at yield was found to be insignificant at a 90% confidence level. The contributions of these variables were therefore pooled with the error term to establish the relative contributions of pressure and temperature. (Figure 12) It is clear that pressure is the dominant variable influencing the flexural stress at yield. The effect of temperature is more pronounced for the yield strength in view of adhesion between the phlogopite and the LLDPE being of greater importance for properties tested at large deformations.

6.3.2 Tensile properties

Figure 13 shows the ANOVA results for the tensile properties of the composite.

Tensile tests have more value where the adhesion of the binder to matrix material is of importance. Figure 13 and Table A4 show that none of the variables investigated played a significant role in determining the Young's modulus. Although pressure was the

dominant variable it was still insignificant even if all the other variables are pooled with the error term. This implies that the moulding temperatures and times investigated were sufficient to ensure the attainment of ultimate properties for the composite.

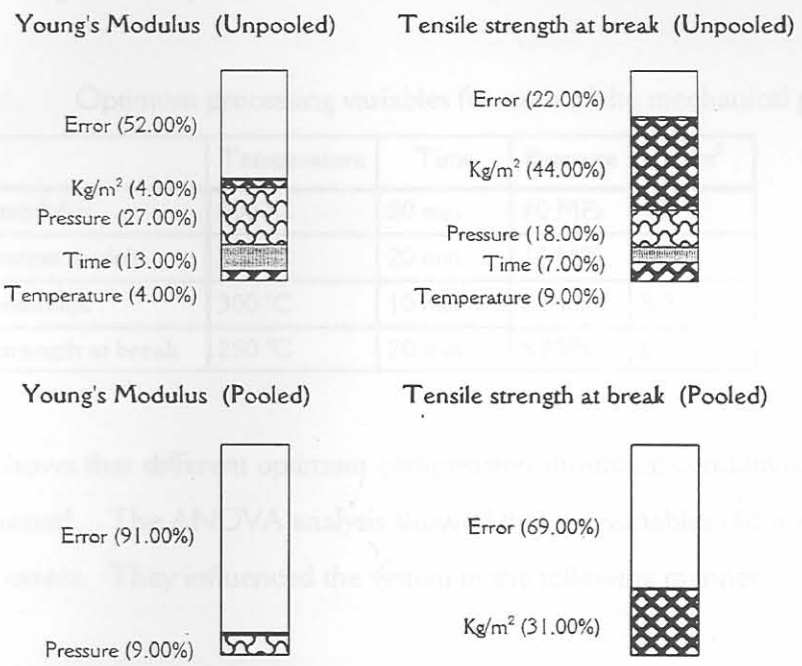

Figure 13: Relative contribution of processing variables towards the tensile properties (pooled and unpooled)

The tensile stress-at-break is a good indication of the adhesion properties of the composite. Figure 13 shows that only the mass of material used per unit area influenced this property.

For the present processing conditions, the optimum amount of material for tensile stress at yield was at the minimum value tested, 5 kg/m^2 material per sheet. (Table 8) Only the flexural modulus and tensile strength of the composite are dependant on the thickness of the composite (mass per area used) as the material has a laminar structure and is therefore inhomogeneous. The flexural modulus of the material is increased when more phlogopite flakes align in plane of the composite; more plates in plane of the composite is the result

of a higher amount of material per unit area. The tensile strength of the composite is decreased by an increase in thickness of the composite. This is probably due to inhomogeneity in the thicker composites owing to pressure transmission and heat transfer effects. Visual inspection of the thick samples showed poor bonding at the centre. This may imply that heat transfer from the heated press to the material was the limiting factor. Proper melting and compaction of the material was not achieved for the thick samples.

Table 8: Optimum processing variables for each of the mechanical properties

	Temperature	Time	Pressure	kg/m^2
Flexural modulus	300 °C	20 min	10 MPa	10
Flexural stress at yield	300 °C	20 min	10 MPa	5
Young's modulus	300 °C	10 min	8 MPa	8.3
Tensile strength at break	250 °C	20 min	8 MPa	5

Table 8 shows that different optimum compression moulding conditions exist for each property tested. The ANOVA analysis showed that the variables did not contribute to the same extent. They influenced the system in the following manner:

- **Temperature.** Higher temperatures will reduce the viscosity of the polymer binder improving its fluidity. This aids wet-out and compaction.
- **Time.** Enough time should be allowed for sufficient heat transfer to take place to ensure complete melting of the binder.
- **Pressure.** Sufficient pressure must be applied to ensure efficient compaction. Pressure aligns the particles such that their greatest area is exposed perpendicular to the applied pressure. Misalignment will result in the formation of voidage which will cause a reduction in mechanical properties
- **Mass per unit area.** The mass of material used in the mould will ultimately determine the thickness of the composite. The thickness of the sheet will influence the heat transfer from the mould to the inner parts of the composite.

7. YOUNG'S MODULUS AND VOIDAGE

When the large panel potential application of this material is considered, the most appropriate property would be the flexural modulus. This effectively measures the material's stiffness with respect to bending deformation. However, the bending modulus is of the same order of magnitude as the Young's modulus and follows the same trend. [36] The focus in this study will therefore be on the Young's modulus.

In Chapter 3 the following formulation variables were identified attributing to the properties of a composite:

- the shape and orientation of the reinforcing agent
- particle size and distribution
- concentration of polymer
- the degree of interfacial adhesion.

Each of these affect the composite in a different manner, as described earlier. The ANOVA results presented in the preceding sections revealed that:

- particle size contributed the most towards the Young's modulus (32%), with the wt% polymer second (16%). The contributions were, however, small compared to the error.
- the modification technique used contributed 11% towards the average performance, with even less significance than the other parameters tested.
  If these are compared with the results for the flexural modulus, it is evident that the amount of polymer used is the most significant variable.
- concerning the preparation variables, pressure contributed the most towards the Young's modulus.
  Compared with the results for the flexural modulus, it is evident that pressure is the most important preparation variable. Particle shape will ultimately influence the ability for good packing of particles in the composite. Bad packing will result in a

in a high voidage, especially when the percentage polymer is low. Using a high pressure during manufacture will help reduce the voidage caused by poor packing.

The ideal model to predict the Young's modulus of a systems should therefore:

- include the amount of binder resin (polymer)
- take into account the particle size or aspect ratio of the filler
- account for packing inefficiencies and mis-alignment of the filler
- make provisions for the adhesion efficiency between the filler and binder resin.

In the proposed model the following assumptions are made:

- the binder resin (LLDPE) and filler (phlogopite) are linear elastic
- the plates are rectangular and have uniform width and thickness.
  Deviations from this assumption are accounted for by postulating a voidage for the composite. It is evident that when the volume fraction polymer is zero, the voidage is not zero.
- the plates are aligned in a plane parallel format
  The compression moulding technique ensures proper alignment. Figure 14 shows the SEM photo of a composite comprising 8% LLDPE. Note that the binder was etched away to reveal the orientation.

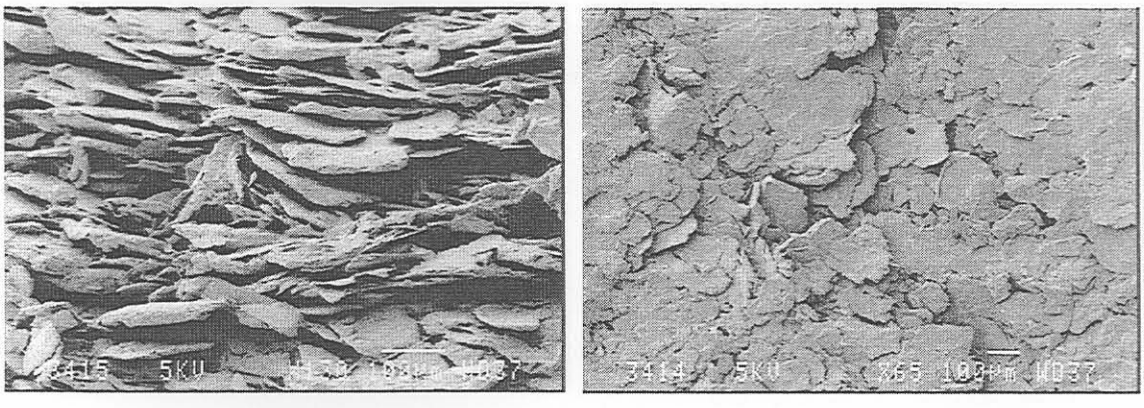

A: Side view B: Top view

Figure 14: Side and top view of a LLDPE / phlogopite composite, containing 8% LLDPE

- there is perfect bonding between the resin and the filler.

in a high voidage, especially when the percentage polymer is low. Using a high pressure during manufacture will help reduce the voidage caused by poor packing.

The ideal model to predict the Young's modulus of a systems should therefore:

- include the amount of binder resin (polymer)
- take into account the particle size or aspect ratio of the filler
- account for packing inefficiencies and mis-alignment of the filler
- make provisions for the adhesion efficiency between the filler and binder resin.

In the proposed model the following assumptions are made:

- the binder resin (LLDPE) and filler (phlogopite) are linear elastic
- the plates are rectangular and have uniform width and thickness.
  Deviations from this assumption are accounted for by postulating a voidage for the composite. It is evident that when the volume fraction polymer is zero, the voidage is not zero.
- the plates are aligned in a plane parallel format
  The compression moulding technique ensures proper alignment. Figure 14 shows the SEM photo of a composite comprising 8% LLDPE. Note that the binder was etched away to reveal the orientation.

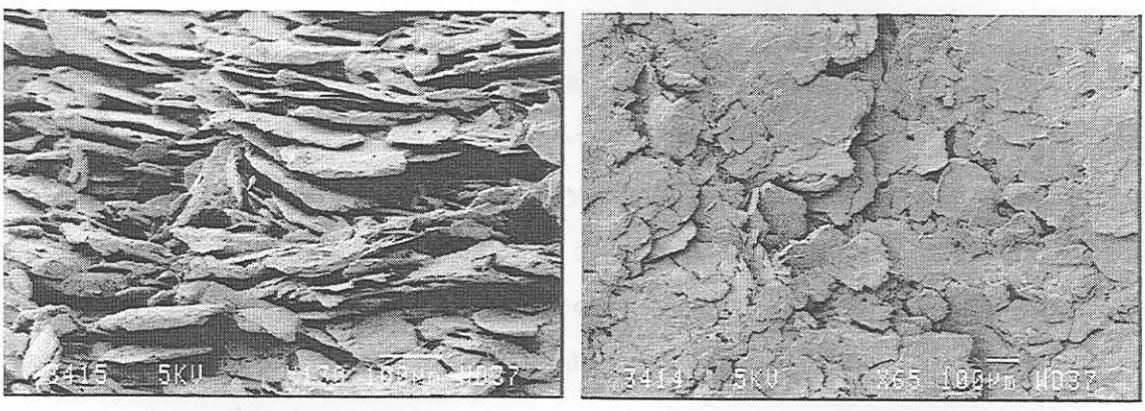

A: Side view B: Top view

Figure 14: Side and top view of a LLDPE / phlogopite composite, containing 8% LLDPE

- there is perfect bonding between the resin and the filler.

of the flakes. The maximum voidage is defined as the fraction free volume when this bed is densely compacted. It can be calculated using Equation 9.

$$\phi_m = 1 - \frac{V_{particle}}{V_{apparent}} \tag{9}$$

For the case of a single platelet with its associated void volume, it can be expressed in terms of projected surface areas:

$$\phi_m = \frac{A_v \times t}{(A_v + A_{pa}) \times t}$$

where t is the plate thickness.

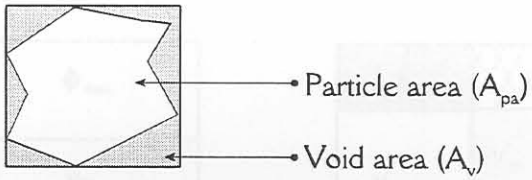

7.1.2 Total voidage

For a composite that contains matrix material there are two limiting situations. If the polymer during processing has a very low viscosity it will first fill the empty space available. If, however, the viscosity is very high, very little of the voidage will be filled. In practice the voidage of thermoplastic composites depends strongly on the temperature and the pressure applied during sheet manufacture. However, the two limiting situations define upper and lower bounds for the final voidage (See Figure 17).

The voidage, ϕ, of the composite can be calculated from the fraction open volume remaining after polymer has been added to aligned particles at maximum packing density. Consider a unit volume of such a composite as illustrated below. The voidage of such a composite could be modelled using the scheme proposed in Figure 16. It implies a specific

manner in which the resin partially displaces the reinforcement and fills the available void space.

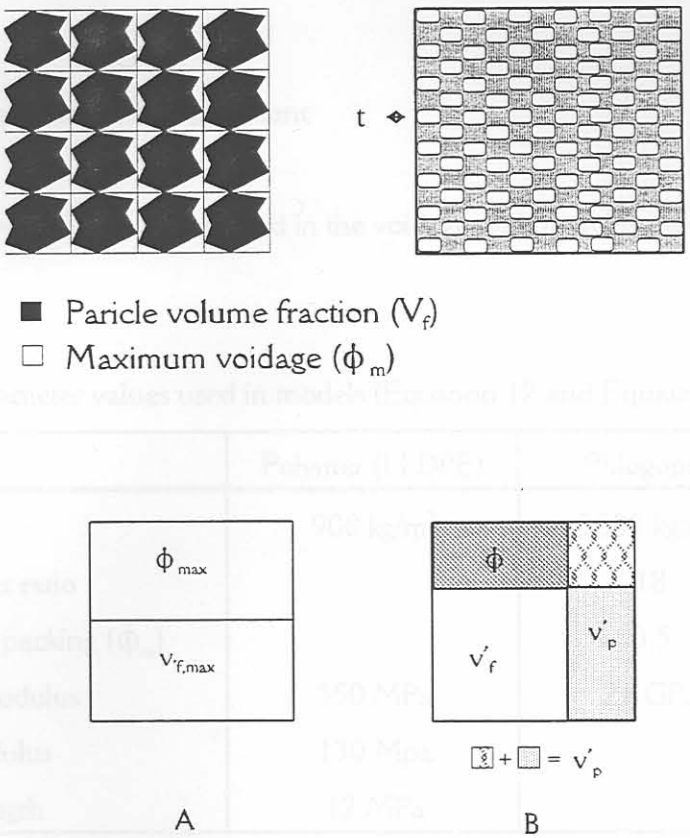

Figure 16: Schematic representation of the void volume in a composite

In this unit volume of composite that contains a volume fraction v'_f of reinforcement, the associated voidage is equal to:

$$\frac{\phi_m}{1-\phi_m} v'_f \tag{10}$$

The sum of the volume fraction must equal unity, i.e.

$$\phi + v'_p + v'_f = 1 \tag{11}$$

Combining these two equations leads to a simple expression for voidage as a function of volume fraction polymer: (A more detailed discussion is presented in Appendix 2)

$$\phi = \frac{(1 - v_p')^2 \phi_m}{1 - v_p' \phi_m} \tag{12}$$

7.1.3 Correlation with experiment

Table 9 shows the parameters used in the voidage and modulus models.

Table 9: Parameter values used in models (Equation 12 and Equation 24)

	Polymer (LLDPE)	Phlogopite
Density	900 kg/m^3	3000 kg/m^3
Plate aspect ratio		18
Maximum packing (ϕ_m)		0.5
Young's modulus	350 MPa	21 GPa
Shear modulus	130 Mpa	
Shear strength	12 MPa	

Figure 17 shows that this model (Equation 12) provides a reasonable fit to the experimental data. It also suggests that the voidage does not depend on the particle size. This is not unexpected since it is known that the density of, for example, a randomly packed bed of spheres is independent of particle size. [37] The maximum packing density does, however, depend on the shape and orientation of the particles in the composite.

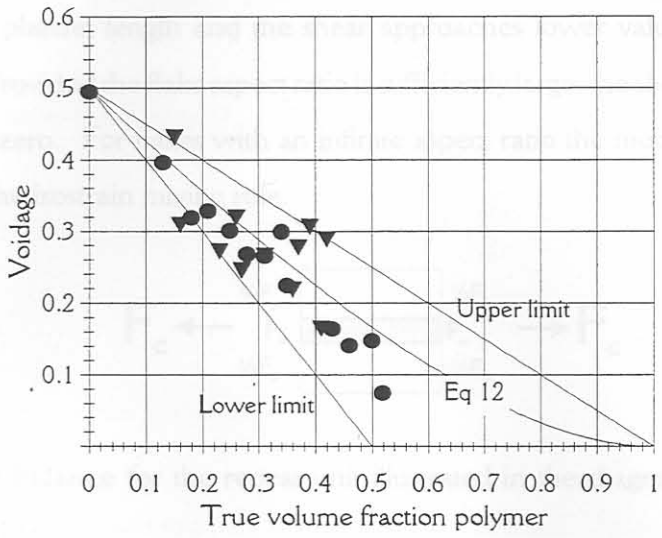

Figure 17: Composite voidage as a function of the volume fraction polymer (V_p). Particle size: ▼: 250-300 μm ● : 125- 80 μm. ϕ_m=0.5

7.2 Modelling the Young's modulus

Consider a system where the reinforcements are rectangular platelets aligned parallel to the applied force. The dashed lines in the diagram below define a repeat unit that is representative of the composite.

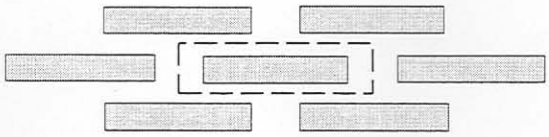

It is assumed that the average strain will be uniform when a force, F, is applied to the composite. Cox [38] proposed that the stress in the polymer layer is transferred to the

flakes via a shear mechanism. Since the plates are discontinuous the shear force will be a maximum at the edges of the individual particles. Stress transfer occurs progressively along the platelet length and the shear approaches lower values at the middle of the platelet. Provided the flake aspect ratio is sufficiently large, the shear will actually decrease to almost zero. For flakes with an infinite aspect ratio the modulus of the composite is given by the isostrain mixing rule.

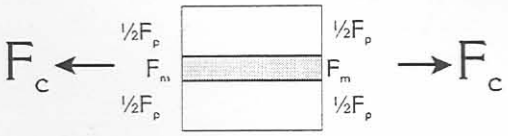

The force balance for the repeat unit illustrated in the diagram above, is as given by Equation 13:

$$F_c = F_m + F_p \tag{13}$$

From the previous argument, stating that stress is transferred by a shearing mechanism, it follows that the total stress cannot be transferred between the polymer and the plates and the load carried by the plates will therefore be lower than predicted by the isostrain mixing rule.

7.2.1 Tensile force in the platelet

With the particles being discontinuous, the force acting on the platelet will be a function of the length of the particle. The nett result is that the displacement in the particle will also vary with length. Thus F_m, in Equation 13, describes the average force acting on the platelet.

The tensile stress in the platelet, as a function of distance from the edge of the platelet, x, is described by Hooke's law as $\sigma_f(x) = \frac{du}{dx} E_m$ The corresponding force acting on the platelet (with area $A_t = tW$) is therefore:

$$F_m(x) = E_m(tW)\frac{du}{dx} \tag{14}$$

7.2.2 Shear in the polymer

Perfect bonding between the two phases is assumed. Thus the displacement of the polymer layer is restrained by the platelet. The result is a shear force in the polymer which reaches a maximum at the edges of the platelet. The tensile force transmitted to the particle will therefore be a minimum at this point. Depending on the aspect ratio, a maximum value is reached at some distance along the platelet.

If the displacement of the polymer were ν, at distance x, in the absence of the particle and the displacement of the particle is u (at distance x, from the edge), the displacement of the polymer will have been restrained by the distance ω. The shear force in the polymer therefore causes a shear strain γ, associated with the displacement, ω. Figure 18 illustrates the situation as described above.

The displacement due to the shear stress $d\tau$, is: $\omega = \frac{S}{2}\tan\gamma$, for small values of γ, ω becomes: $\omega = \frac{S}{2}\gamma$. Hooke's law for shear deformation can be used to express the shear deformation, i.e. the angle γ, as $\gamma = \frac{\tau}{G_p}$.

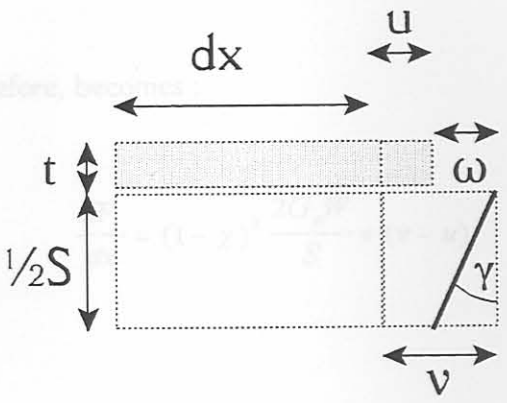

Figure 18: Shear strain in the polymer phase due to the restraining action of the platelet

The shear stress, τ, acts over the area dA_f, and the shear force is expressed as: $dF_s = \tau dA_f$, with $dA_f = Wdx$

With $\omega = v - u$, the shear force can now be expressed as:

$$\frac{dF_s}{dx} = \frac{2G_p W}{S}(v - u) \tag{15}$$

The stress transfer will also be influenced by the voidage in the polymer phase, χ. The voidage will influence the area over which the shear force acts and is therefore $dx(1-\chi)$. The spacing between the plates is proportional to the volume fraction polymer and the true distance is therefore $\frac{S}{(1-\chi)}$, taking the voidage into account. The shear modulus of the polymer will also be reduced by the factor $(1-\chi)$. The voidage in the polymer

phase can be calculated relative to the composite voidage, ϕ, as $\chi = \frac{\phi}{v_p(1-\phi)+\phi}$.

Equation 15, therefore, becomes :

$$\frac{dF_s}{dx} = (1-\chi)^3 \frac{2G_pW}{S} \times (v-u) \tag{16}$$

7.2.3 Average tensile force in the particle

Equations 14 and 16 can be combined by noting that $2dF_s = -dF_m$ and that $\frac{dv}{dx} = \varepsilon$,

where the strain, ε, in the polymer, in the absence of the platelet, is constant. The result is:

$$\frac{dF_m^2}{d^2x} = \frac{(1-\chi)^3 4G_pW}{S} \times \left(\frac{F_m}{E_m tW} - \varepsilon \right) \tag{17}$$

Equation 17 can be solved by using the Laplace transformations, with boundary conditions are $F_m = 0$ when $x = 0$ and $F_m = 0$ when $x = D$. After some mathematical manipulation the result is (See Appendix 2):

$$F_m(x) = E_m tW\varepsilon \left(1 - \frac{\cosh(\mu \frac{D}{2} - \mu x)}{\cosh(\mu \frac{D}{2})} \right) \tag{18}$$

where :

$$\mu = \sqrt{\frac{(1-\chi)^3 4G_p}{SE_m t}}$$

The average force F_m can be found by integrating Equation 18 over the length D and dividing by the total length D. The result is:

$$F_m = E_m t W \varepsilon \left(1 - \frac{\tanh(\varphi)}{\varphi}\right) \tag{19}$$

where:

$$\varphi = \sqrt{\frac{(1-\chi)^3 G_p D^2}{S E_m t}} \tag{20}$$

The aspect ratio of the flakes is given by $\alpha = \frac{D}{t}$. The ratio $\frac{t}{S}$ can be expressed in terms of volume fractions. This reduces Equation 20 to:

$$\varphi = \alpha \sqrt{\frac{(1-\chi)^3 G_p}{E_m} \times \frac{v_f}{1-v_f}} \tag{21}$$

7.2.4 Composite modulus

For the composite Equation 13 can be expressed as:

$$\frac{F_c}{A_c} A_c = F_m + \frac{F_p}{A_p} A_p \tag{22}$$

The area occupied by the plates is: $A_m = t \times W$ and the area of the polymer is: $A_p = s \times W$, where W is the width of the plates. The total area over which force F_c is applied is: $A_c = (s+t)W$. Equation 22 can therefore be written as:

$$\sigma_c = \frac{F_m}{(S+t)W} + \frac{S}{(S+t)} \sigma_p \tag{23}$$

With F_m given by Equation 19 and the ratios $\frac{t}{s+t}$ and $\frac{s}{s+t}$ the volume fraction platelets ,v_f and polymer, v_p respectively. Noting that the Young's modulus of an elastic material is given as $E = \frac{\sigma}{\varepsilon}$ and assuming that the composite is under a uniform strain, ε, Equation 23 can be reduced to:

$$E_c = v_f E_m MRF + v_p E_p \tag{24}$$

where the modulus reduction factor (MRF) is given by:

$$MRF = \left(1 - \frac{\tanh(\varphi)}{\varphi}\right) \tag{25}$$

The result is similar to that of Cox [38] as modified by Padawer and Beecher [27], apart from the correction for voidage. This correction is critical as it provides the correct limit of zero modulus for a particulate composite in the absence of matrix. Figure 19 graphically compares the modulus correction factors.

7.2.5 Comparison with experiment

Figure 20 shows the results obtained for the Young's modulus of the composites, as described in Section 5.4, and the predicted Young's modulus, calculated using Equation 24 together with Equation 12 for voidage. The predicted modulus values are very close to the experimentally measured ones. This confirms that the present model overcomes the drawbacks of previous models for the case where the matrix is present in very low concentrations. Figure 21 compares the new model with previous ones. It predicts much lower values for the Young's modulus. For high volume fraction polymer its predictions are similar to those of the model by Padawer and Beecher [27] and the isostrain mixing rule.

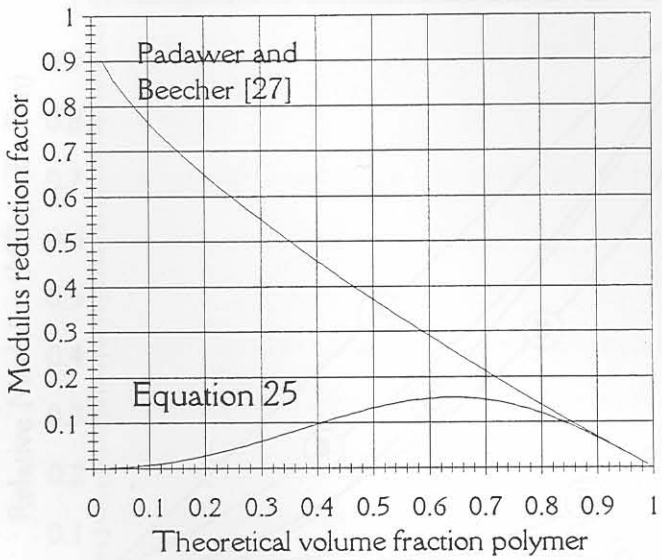

Figure 19: Comparison of the modulus reduction factors of Cox[38], as modified by Padawer and Beecher [27] with Equation 25 together with Equation 12

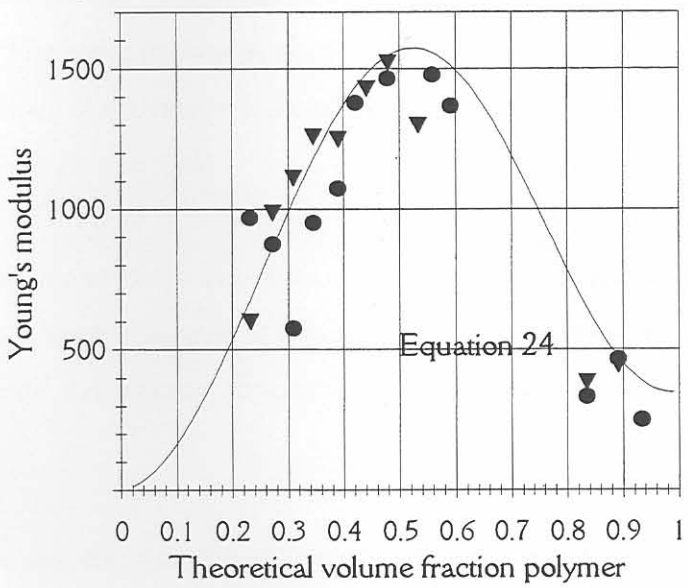

Figure 20: Measured modulus (● 125 - 180 μm) and the modulus calculated with Equation 24. Parameter values are given in Table 9

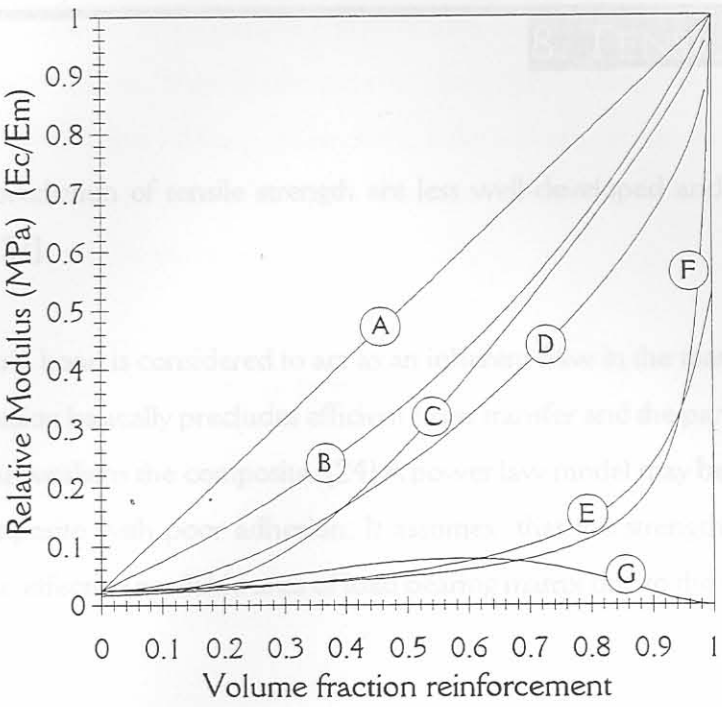

Figure 21: The predicted variations of the tensile modulus of a composite: A: Isostrain (1A), B: Jacquet el al. (4) , C: Padawer and Beecher (5A), D: Lusis et al. (5B), E: Kerner and Lewis (6), F: Isostress (1B), G: Equation 24 Quantities in brackets indicate the equation numbers in the main text.

8. TENSILE STRENGTH

Models for the prediction of tensile strength are less well-developed and generally give poor predictions. [24, 27]

The particle-matrix bond is considered to act as an inherent flaw in the material when adhesion is poor. Poor adhesion basically precludes efficient stress transfer and the particle can therefore be seen as a void that weakens the composite. [24] A power law model may be used to describe the strength of a composite with poor adhesion. It assumes that the strength of the composite is determined by the effective available area of load bearing matrix due to the presence of the filler. [24]

$$\sigma_c = \sigma_p(1 - av_f^b) \tag{26}$$

Here a and b are constants that depend on the particle shape and orientation. These are the most important variables that determine the tensile strength of particular filled systems. [24] The tensile strength generally increases with a decrease in particle size as smaller particles provide a greater interfacial area. The result is a more effective interfacial bond. Particle size is also related to the flaw size dependence of the material, therefore the probability of finding a large flaw decreases with decreasing particle size. [24]

Irregular fillers are expected to weaken the composite owing to high stress concentrations around the sharp edges. A stress concentration factor can also be introduced to take into account the reduction in strength due to stress concentrations caused by irregular shapes.

$$\sigma_c = \sigma_p(1 - av_f^b)K \tag{27}$$

It is clear that the available models only predict an upper limit for the strength of the composite and that stress concentrations will lower these values by an undetermined amount. [24]

The model by Padawer and Beecher [27] for the Young's modulus was described earlier. They also postulated that the strength of the composite can be modelled in a likewise manner. If the

maximum calculated stress in the particle is greater than the tensile strength of the particle, failure will be due to flake fracture. If the maximum calculated shear strength in the matrix exceeds the shear strength of the polymer, failure will be due to flake pull-out. It was found, however that the latter case is predominant in most cases. [27] The above situation, for the tensile strength in the plane of orientation, can be described by equation 28.

$$\sigma_c = v_p \sigma_p + K_3' \tau_p MPF \tag{28}$$

where

$$MPF = v_m \left(\frac{\alpha}{u}\right)\left(\frac{1}{\tanh(u)} - \frac{1}{u}\right)$$

$$u = \alpha \left(\frac{G_p v_f}{E_m (1 - v_f)}\right)^{\frac{1}{2}}$$

Apart from the deviations from ideal behaviour, which are accounted for by the factors K_3' (Equation 28) and K (Equation 27), both suffer the same limitation as do the models for Young's modulus. That is, the accuracy of predicting the tensile strength of the composite when the volume fraction polymer is approaching zero becomes very poor. Experimental data for tensile strength and stress at maximum load (in the plane of orientation) are presented in Figure 22, for LLDPE and phlogopite composites, as described in previous sections.

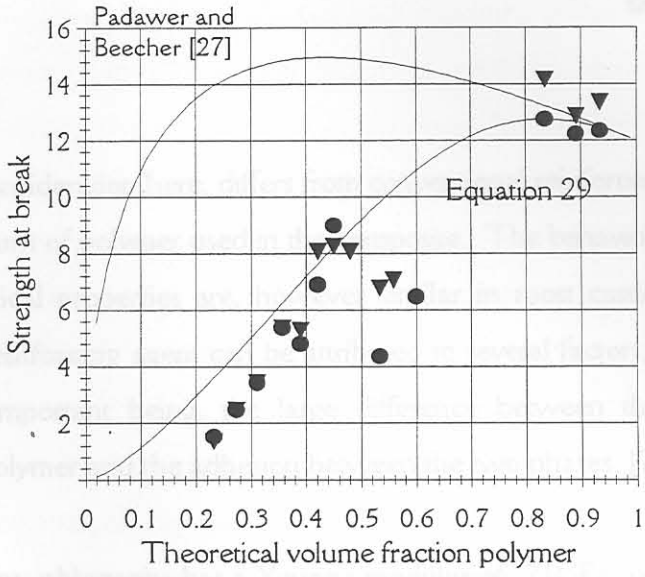

Figure 22: Maximum stress and stress at break. ■ Stress at break, 125 - 180μm, • Maximum stress, 125 - 180 μ, ▼, Maximum stress, 250 - 300 μm.

It is evident from the graph that equation 28 does not accurately describe the tensile strength of the composite at low volume fractions polymer. Accuracy can however be improved by realising that the voidage of the composite influences the effective available area of load bearing matrix. The matrix performance factor is therefore further reduced by the factor $(1-\chi)$, with χ defined as in section 6.4.2. The available area in the polymer phase is also reduced by the same amount. Equation 28 can therefore be modified to be:

$$\sigma_c = \left(v_p \sigma_p + K_3' \tau_p MPF\right)(1-\chi) \qquad (29)$$

Figure 22 shows a comparison of Equation 29 with the present experimental data. A value for K_3' of 0.75 gives a reasonable fit. This modification resulted in a significant improvement in the correlation of the tensile strength and maximum stress, at low volume fraction polymer.

9. Discussion

The composite under consideration here, differs from conventional reinforced polymers mainly with respect to the amount of polymer used in the composite. The behavior of the composite with respect to mechanical properties are, however similar in most cases. Normally the reinforcing action of a reinforcing agent can be attributed to several factors, as pointed out in Chapter 3, the most important being, the large difference between the stiffness of the reinforcement and the polymer and the adhesion between the two phases. [7]

Considering the first point, phlogopite has a Young's modulus of 21GPa, while LLDPE has a Young's modulus of only 0.35GPa. One can therefore expect that the large difference between these values would cause a considerable stiffening effect in the polymer. The maximum stiffness that can be obtained is, however, not only dependant on the higher stiffness of the reinforcement. Several other factors also influence the stiffening effect of the reinforcement. These were pointed out in Chapter 3 as the size and shape of the reinforcement [12], the particle size [13] and distribution [14] and the concentration of the reinforcement. [13]

A somewhat surprising result is that of the effect of interfacial adhesion. The analysis of variance, as well as the initial scoping experiments (Chapter 6) revealed that the use of techniques normally effective in improving the adhesion of a non-polar polymer onto a polar mica surface was relatively unimportant compared to the other factors investigated. SEM micrographs also revealed that even with no modification to the polymer, good adhesion is obtained, evident from the thread-like edges around the particles after break (Figure 15).

From the results obtained in Chapter 6 in can be seen that in terms of the Young's modulus particle size and weight percentage polymer are indeed the most important parameters. The effect of polymer content was however slightly misleading due to non-linear effects not accounted for in the analysis of variance. Chapter 3 referred to the filler and mastic theory with regards to reinforced polymers [14]. The stiffening effect of the filler can therefore be accounted for not only

by the packing efficiency, but also to the amount of polymer that is able to coat the particles. This coating around he particles effectively binds the particles together. If this coating is therefore discontinuous, or not adhere strongly to the surface, the results would be a material where the full potential reinforcing effect of the filler is not utilized. In the model for Young's modulus presented in Chapter 7, this effect was accounted for by modeling a voidage for the composite, which is dependant on the volume fraction polymer in the composite. In other words, if complete wet-out is not possible, because too little binder is present, the result would be the formation of voids, which will reduce the modulus of the composite.

Other effects that were not explicitly investigated was the particle size distribution of the reinforcement. In can, however, be expected that a distribution of particle sizes would result in an increase in the stiffening effect of the filler, as the smaller particles can increase the packing efficiency by packing in between the larger particles (filler theory). In the model for Young's modulus (Chapter 7) as well as the model for tensile strength (Chapter 8) the effect of particle size distribution would be accounted for in the maximum packing factor for that specific filler gradation.

In Figure 20 the concentration dependance of Young's modulus, predicted by the proposed model, compared with experimental results is shown. One important observation is the observed maximum value for modulus. This maximum shows that even with the large difference between the stiffness of the reinforcement and the binder, the maximum stiffness of the composites is considerably less than that of the filler. The maximum is strongly dependant on the aspect ratio of the reinforcement. It should therefore also be noted that as the aspect ratio is increased the model ultimately approaches the isostrain model, with the implication that the reinforcement is monolithic.

Other important aspects of this specific composite are the processing conditions that can greatly influence the modulus and tensile strength. Poor compaction of the filler and poor coating by the binder will result in excessive voidage, which will result in a lower than expected modulus and strength.

10. Conclusions

Phlogopite is brown mica that is produced as a mining by-product at Phalaborwa. Its availability and low cost make it a desirable filler and extender for polymer based composites. This study investigated the mechanical properties of compression moulded LLDPE / phlogopite sheets.

The Taguchi method was used to separately investigate the effects of composition and processing variables on the mechanical properties of compression moulded sheets. The composition variables considered were: particle size, polymer content and type of polymer modification. With respect to main effects (Young's Modulus) the factors particle size (32%) and polymer content (16%) were found to be the most important. However, these contributions to explaining the observed variance were small compared to the error term. The modulus showed a maximum value at a polymer content of approximately 20% by mass.

The processing variables considered were: holding pressure, mould temperature, moulding time and the amount of material moulded per unit area. Concerning the preparation variables, pressure contributed the most towards the Young's modulus (27%), although the contribution was small compared to the unexplained error. Pressure was a more important factor for the flexural modulus (70%). The highest tensile strength was obtained at the minimum value of 5 kg/m^2 material used.

For the present thermoplastic sheet composites it was not possible to achieve complete densification of the sheet material. The residual voidage was observed to depend on the amount of binder used. It also correlated with the maximum packing density of the pure reinforcement. The observed densities were intermediate to the theoretical upper and lower limits corresponding to complete wet-out and non-penetration of the filler bed.

A theoretical model for the Young's modulus, in the plane of reinforcement orientation, was derived. It is similar to the Cox [38], as modified by Padawer and Beecher [27] model. However, it also incorporates the effect of composite voidage on mechanical properties. Unlike other models,

it correctly predicts the loss of modulus in the limit of zero binder. Good agreement was found between the predictions of this model and experimental measurements.

Compared to other models the new model predicts significantly lower values for the Young's modulus. At high volume fractions binder its predicted values are similar to those of the model by Padawer and Beecher [27]as well as the isostrain mixing rule.

A similar approach was used to correlate the composite tensile strength. Again a good agreement was found between the model and the experiment.

11. References

1. Sims, C. *Mica - Building a future on dry ground.* Industrial Minerals. (1997)
2. Davis, L.L. *Mica.* Minerals Review. Vol 73 pp 113 - 114 (1994)
3. The Quinto Mining Corporation. *Products.* (1998) [On-line] Available: http://www.quintomining.com/products.html
4. GunPatroy (Pty) Ltd. *Mica and its applications* (1999) [On-line] Available: http://www.cirrusweb.com/grgroup/mica.html
5. Usifer, D. Fajaro, W. *Mica and its effect in polyolefin compounds.* Society of Plastics Engineers. Polyolefins XI International Conference. (1999)
6. Bayles et al. *Method for producing mica based insulation.* US Patent no 4,107,358. (1978)
7. Gachter, R. Muller, H. *Plastics Additives Handbook.* Fillers and Reinforcements, Chapter 9. 2nd edition. Hanser Publishers, New York. Pp 410-525 (1987)
8. Jarvela, P.A. Jarvela, P.K. *Multicomponent compounding of polypropylene.* Journal of Materials Science. Vol 31 pp 3853 - 3860 (1996)
9. Baral, D. De, P.P. Golok, B. Nando, B. *Thermal characterization of mica-filled thermo plastic polyurethane composites.* Polymer Degradation and Stability. Vol 65 pp 47 -51 (1999)
10. Kozlowski, R. Mieleniak, B. Helwig, M. Przepiera, A. *Flame resistant lignocellulosic-mineral composite particle boards.* Polymer Degradation and Stability. Vol 64 pp 523 - 528 (1999)
11. Dodds, N. Gibson, A.G. Dewhurst, D. Davies, J.M. *Fire behaviour of composite laminates.* Composites: Part A. Vol 32 pp 689 - 702 (2000)
12. Xanthos, M. Faridi, N. Li, Y. *Processing/Structure relationships of mica-filled PE-films with low oxygen permeability.* International Polymer Processing XIII. Vol 1 pp 58 - 66 (1998)
13. Anderson, L.L. *A predictive model for the mechanical behaviour of particulate composites.* Polymer Engineering and Science. Vol. 28 (8) pp 522 - 528 (1988)

14. Sidess, A. Holdengraber, Y. Buchman, A. *A fundamental model for prediction of optimal particulate composite properties.* Composites. Vol. 24 (4) pp 355 - 360 (1993)

15. Nagay,N. Kusefoglu,S. Erman, B. Journal of Applied Polymer Science. Vol 66 pp 1943 - 1952 (1997)

16. Kovačevic, V. Lučic, S. Cerovečki, Z. *Influence of filler surface pre-treatment on the mechanical properties of composites.* International Journal of Adhesion and Adhesives. Vol 17 pp 239 - 245 (1997)

17. Busigin, C. Martinez, G.M. Woodhams, R.T. *Factors affecting the mechanical properties of mica-filled polypropylenes.* Polymer Engineering and Science. Vol 23 (14) pp 766 - 770 (1983)

18. Newman, S. Meyer, F.J. *Mica composites of improved strength.* Polymer Composites. Vol 1 (1) pp 37 - 43 (1980)

19. Inubushi, S. Ikeda, T. Tazuke, S. *Aminimide-cured epoxy resins as surface modifiers for mica flakes in particulate-reinforced thermoplastics.* Journal of material Science. Vol 23 pp 535 - 540 (1988)

20. Debnath, S. De, S.K. Khastgir, D. *Effect of Silane coupling agent on vulcanization, network structure, polymer-filler interaction, physical properties and failure mode of mica-filled styrene-butadiene rubber.* Journal of Materials Science. Vol 22 pp 4453 - 4459 (1987)

21. Gosh, P. Chattopadhyay, B. Sen, A.K. *Modification of low density polyethylene (LDPE) by graft copolymerization with some acrylic monomers.* Polymer. 39 pp 193 - 201 (1998)

22. United Minerals Corporation. *The Uni-Kote® Process.* (1997) [On-line] Available: http://www.ceramics.com/aim/unikote.html

23. Meddad, A. Fisa, B. *Filler- matrix debonding in glass bead-filled polystyrene.* Journal of Materials Science. Vol 32 pp 2013 - 2024 (1997)

24. Ahmed, S. Jones, F.R. *A review of particulate reinforcement theories for polymer composites.* Journal of Materials Science. Vol 25 pp 4933 - 4942 (1990)

25. Bhattacharya, A. *Radiation and Industrial polymers.* Progress in Polymer Science. Vol 25 pp 371 - 401 (2000)

26. Wakeman, M.D. Cain, T.A. Rudd, C.D. Brooks, R. Long, A.C. *Compression moulding of glass and polypropylene composites for optimized macro- and micro- mechanical properties - Commingled glass and polypropylene.* Composites Science and Technology. Vol 58 pp 1876 - 1898 (1998)

27. Padawer, G.E. Beecher, N. *On the strength and stiffness of planar reinforced plastic resins.* Polymer Engineering and Science, Vol 10 (3) pp 185 - 190 (1970)

28. Ward, I.M. Hadley, D.W. *An Introduction to the Mechanical Properties of Solid Polymers.* 1st Edition (1993). Wiley Publishers.

29. Jacquet, E. Trivaudey, F. Varchon, D. *Calculation of the transverse modulus of a unidirectional composite material and of the modulus of an aggregate. Application of the rules of mixtures.* Composites Science and Technology. Vol. 60 pp 345 - 350 (2000)

30. Akiva, U, Itzhak, E. Wagner, H.D. *Elastic constants of three-dimensional orthotropic composites with platelet / ribbon reinforcement.* Composites Science and Technology. Vol 57 pp 173 - 184 (1997)

31. ASTM D790. Vol 08.01 Plastics(1) 1983. *Standard test methods for Flexural properties of unreinforced and reinforced plastics and electrical insulating materials*

32. ASTM D638. Vol 08.01 Plastics(1) 1982. *Standard test method for tensile properties of plastics*

33. Gammatron (Pty) Ltd. Stokkiesdraai Ave. Erasmusrand Pretoria, South Africa

34. FOSKOR Ltd. P.O. Box 1. Phalaborwa. South Africa

35. Roy, R.K. *A Primer on the Taguchi method.* (1990). 1st edition. Van Nostrand Reinhold - New York.

36. Lussis, J. Woodhams, R.T. Xanthos, M. *The effect of flake aspect ratio on the flexural properties of mica reinforced plastics.* Polymer Engineering and Science. Vol 13 (2) pp 113-145 (1973)

37. Foust, A.S. Wenzel, L.A. Clump, C.W. Maus, L. Anderson, L.B. Principles of unit operations. 2nd Edition. (1980) John Wiley & Sons

38. Cox, H.L. The elasticity and strength of paper and other fibrous materials. British Journal of Applied physics. Vol 3 pp 72 - 78 (1952)

39. Casenave, S. Aït-Kadi, A. Riedl, B. *Mechanical behaviour of highly filled lignin/polyethylene composites made by catalytic grafting.* The Canadian Journal of Chemical Engineering. Vol 74 pp 308 - 315 (1996)

40. Inubushi, S. Ikeda, T. Tazuke, S. *Excellent flexural properties of aminimide-cured epoxy resin as a matrix for mica-dispersed polymer composites.* Journal of Material Science. Vol 23 pp 1182 - 1188 (1988)

41. Gargassi, F. Morra, M. Occhiello, E. *Polymer Surfaces - From Physics to Technology.* Chapter 10. Chichester : Wiley (1996)

12. APPENDIX 1

Composition variables

-

Table A1: Average performance used to determine optimum conditions

Factor	Level	Measured value (MPa)			
		Flexural modulus	Flexural stress at yield	Young's modulus	Tensile strength at break
Polymer type	LLDPE	*5594*	42.21	4735.8	7.07
	Irradiated	3294	27.79	3346	5.2
	Fusabond	5031.7	*45.05*	*4953.4*	6.21
	AA & LLDPE	4258	33.54	4474.8	*7.23*
% Polymer	8%	623.7	12.5	3168	1.07
	14%	5192	35.51	4920.6	7.27
	20%	*6842*	48.97	*5172*	*8.92*
	24%	5520	*51.61*	4249.4	8.45
Particle size	90	3760	35.67	3101.6	4.86
	125	4098	33.73	3840	6.82
	180	5109	35.71	*6043.2*	*7.32*
	250	*5210*	*43.48*	4525.2	6.71

Table A2: Variance ratios at a 10% level of significance

	Flexural properties				Tensile properties			
	Modulus		Stress at Yield		Modulus		Stress at break	
	Unpooled	Pooled	Unpooled	Values	Unpooled	Pooled	Unpooled	Pooled
	F= 3.3	F= 2.81	F= 3.3	not pooled	F= 3.3	F= 2.6	F= 3,3	F= 2.6
Polymer type	4.1	2.9	24		0.5	Pooled	0.9	Pooled
wt% Polymer	30.2	21.8	121.8		0.8	Pooled	13.6	13.3
Particle size	2.2	Pooled	7.1		1.6	0.97	1.2	Pooled

Preparation variables

Table A3: Average performance used to determine optimum conditions.

Variable	Level	Measured value (MPa)			
		Flexural modulus	Flexural stress at yield	Young's modulus	Tensile strength at break
Temperature (°C)	150	7115	60.45	6899	8.7
	200	7773	70.61	6853	11.28
	250	7463	70.04	6924	**11.75**
	300	**8185**	**84.05**	**7510**	9.85
Time (min)	5	7297	68.9	6744	9.77
	10	6905	69.17	**7545**	10.53
	15	7485	70.35	6447	9.27
	20	**8822**	**76.73**	7450	**12**
Pressure (MPa)	5	5037	55.7	7262	8.53
	6.5	7786	74.3	6185	9.54
	8	7493	71.05	**7992**	**13.1**
	10	**10193**	**84.1**	6747	10.4
Mass (g)	150	8002	**79.86**	6671	**14.76**
	200	6603	66.04	7257	9.12
	250	7073	66.08	**7280**	7.6
	300	**8831**	72.57	6978	10.09

Table A4: Variance ratios at a 10% level of significance

	Flexural properties				Tensile properties			
	Modulus		Stress at Yield		Modulus		Stress at break	
	Unpooled	Pooled	Unpooled	Pooled	Unpooled	Pooled	Unpooled	Pooled
	F= 5.3	F= 5.3	F= 5.3	F= 2.8	F= 5.3	F= 2.6	F= 5,3	F= 2.6
Temperature	5.6	5.6	4.8	3.8	0.1	Pooled	0.4	Pooled
Time	18.4	18.4	0.7	Pooled	0.3	Pooled	0.3	Pooled
Pressure	115.9	115.9	7.3	5.6	0.5	1.5	0.8	Pooled
Mass	25.6	25.5	2.1	Pooled	0.1	Pooled	2	3.2

Densities and voidage

Table A5 : Density and voidage

wt% polymer	theoretical density kg/m^3	Particle size range			
		125 - 180 µm		250 - 300 µm	
		Density kg/m^3	Voidage	Density kg/m^3	Voidage
0	3000	1515	0.49		
8	2528	1527	0.39	1746	0.36
10	2432	1657	0.32	1381	0.32
12	2344	1575	0.33	1705	0.31
14	2261	1581	0.3	1705	0.28
16	2185	1598	0.27	1487	0.29
18	2113	1552	0.27	1550	0.27
20	2046	1586	0.22	1597	0.22
22	1982	1389	0.01	1655	0.17
24	1923	1607	0.16	1388	0.32
26	1867	1604	0.14	903	0.17
28	1815	1679	0.07	1259	0.45
30	1765	1504	0.15	1254	0.09

Table A6: Important physical properties of muscovite and phlogopite [18]

Characteristic	Unit	Muscovite	Phlogopite
Specific gravity		2.6 - 3.2	2.6 - 3.2
Hardness	Moh	2.8 - 3.2	2.3 - 3.0
Tensile strength	MPa	17.5	10
Shear strength	MPa	22 - 27	10 - 13
Modulus of elasticity	GPa	14 - 21	14 - 21
Maximum operating temperature	°C	500 - 600	800 - 900

13. APPENDIX 2

Voidage

The composite can be represented by the unit volume shown in the diagram below:

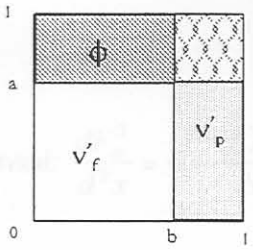

□ + □ = v'_p

The voidage associated with the remaining volume fraction reinforcement, v'_f, is:

$$\frac{v'_f}{(1-\phi_m)}\phi_m = 1-b \qquad 2.1$$

The volume fraction polymer is:

$$v'_p = 1-a \qquad 2.2$$

and the volume fraction reinforcement is:

$$v'_f = ab \qquad 2.3$$

The sum of volume fractions should be equal to one, hence:

$$\phi + v'_p + v'_f = 1 \qquad 2.4$$

Substituting equations 2.1 and 2.2 into equation 2.3 expresses v'_f in terms of v'_p:

$$v'_f = \frac{1-v'_p}{1+\left(\frac{\phi_m}{1-\phi_m}\right)\left(1-v'_p\right)} \qquad 2.5$$

Substituting Equation 2.5 into Equation 2.4 result in the expression for voidage (Equation 12):

$$\phi = \frac{\phi_m(1 - v_p')^2}{1 - \phi_m v_p'} \qquad 2.6$$

Young's modulus

Starting with the second order differential: $\frac{dF_m^2}{d^2x} = \frac{(1-\chi)^3 4G_p}{S} \times \left(\frac{F_m}{E_m t W} - \varepsilon \right)$, which can be solved using Laplace transforms. The equation can be written i.t.o. a few constants: $\frac{dF_m^2}{d^2x} - k_1 F_m + k_2 = 0$, where $k_1 = \frac{(1-\chi)^3 4G_p}{S E_m t}$ and $K_2 = \frac{(1-\chi)^3 4G_p W \varepsilon}{S}$. After taking the Laplace transform, the equation becomes: $S^2 f_m - k_3 - k_1 f_m + \frac{k_2}{S}$, where f_m is now a function of S, in the Laplace domain and $k_3 = F_m'(0)$. The previous equation can then be written as:

$$f_m(S) = \frac{Sk_3 - k_2}{S(S - \sqrt{k_1})(S + \sqrt{k_1})} \qquad 2.7$$

Writing Equation 2.7 in terms of partial fractions yields:

$$f_m = \frac{A}{S} + \frac{B}{\left(S - \sqrt{k_1}\right)} + \frac{C}{\left(S + \sqrt{k_1}\right)} \qquad 2.8$$

with the constants: $A = \frac{k_2}{k_1}$, $B = \frac{\sqrt{k_1}k_3 - k_2}{2k_1}$ and $C = \frac{-\sqrt{k_1}k_3 - k_2}{2k_1}$. The constant k_3 can be determined knowing the end conditions, $F_m(x) = 0$ at $x = 0$ and $x = D$.

Transforming Equation 2.8 back to the x-domain, yields:

$$F_m(x) = A + Be^{\sqrt{k_1}x} + Ce^{-\sqrt{k_1}x} \qquad 2.9$$

The constant k_3 can now be determined as: $k_3 = \frac{k_2}{\sqrt{k_1}} \frac{\left(\cosh\left(\sqrt{k_1}D\right) - 1\right)}{\sinh\left(\sqrt{k_1}D\right)}$. IF the constants A, B, C and k_3 are substituted into Equation 2.9, the result is:

$$F_m(x) = \frac{k_2}{k_1}\left(1 + \frac{\sinh\left(\sqrt{k_1}x\right)\left(\cosh\left(\sqrt{k_1}D\right) - 1\right) - \cosh\left(\sqrt{k_1}x\right)\sinh\left(\sqrt{k_1}D\right)}{\sinh\left(\sqrt{k_1}D\right)}\right) \qquad 2.10$$

By noting that $\sinh\left(\sqrt{k_1}D\right) = 2\sinh\left(\sqrt{k_1}\frac{D}{2}\right)\cosh\left(\sqrt{k_1}\frac{D}{2}\right)$ and that

$2\sinh^2\left(\sqrt{k_1}\frac{D}{2}\right) = \cosh\left(\sqrt{k_1}D\right) - 1$, Equation 2.10 reduces to:

$$F_m(x) = \frac{k_2}{k_1}\left(1 - \frac{\cosh\left(\sqrt{k_1}\frac{D}{2} - \sqrt{k_1}x\right)}{\cosh\left(\sqrt{k_1}\frac{D}{2}\right)}\right) \qquad 2.11$$

To find the average force acting on the particle Equation A5 can be integrated from x = 0 to X = D. This integral is then divided by the length D: $F_{m,avg} = \frac{\int_0^D F_m(x)dx}{D}$.

14. APPENDIX 3

The following table describes the equipment used in this study:

Table A7: Equipment specifications

Equipment	Purpose	Specifications
High speed mixer	Homogenisation of powder mix	*Jones Model HS25 High speed Disperser* **Motor**: 7.5 kW, 380 V **Impleller**: 2x2 blade, the lower following the vessel contour, the upper being flat at right angles. **Vessel**: 25l, without cooling jacket
Heated press	Compression moulding of composite sheets	*20 MPa hydraulic press.* **Bed dimension**: 400x500mm **Temperature range**: Room temperature to 300°C.
Instron	Mechanical testing Tensile (ASTM D638) and flexural (ASTM D790)	Instron Series IX Automated Materials Testing System 1.38 **Capacity**: 5 kN **Cross-head speed**: 5 mm / min, without extensometer 60 mm support span for three point bending tests Samples were obtained by cutting 5 test pieces from each sheet using a standard jig saw

15. Appendix 4

Table A8 lists the results obtained (Young's modulus) from the experiments performed to verify the new model. The columns lists the individual repetitions and the average value at the selected weight percentage polymer used.

Table A8: Results for Young's modulus

Young's modulus (Mpa)

wt % polymer	125-160µm				
	1	2	3	4	Avg
80	138	281	332		250
70	562	437	403		467
60	252	375	371		333
30		1447	1303	1349	1366
28		1426	1559	1446	1478
26	862	851	843		852
24		1119		1095	1107
22	1469	1487	1435		1464
20	1880	1868	1929		1892
18	1349	1614	1063	1486	1378
16	876	1384	899	1138	1074
14	1156	1115	583		951
12	487	398	768	649	576
10	1126	743	755		875
8	1140	478	1283		967

	250-300µm				
	1	2	3	4	Avg
80	131	126	140		133
70	343	489	501		444
60	371	407	376		385
30	744	1052	798	972	892
28	1110	771	1360		1080
26		1403	1195		1299
24	1137	924	943		1001
22	1252	1551	1760		1521
20	1373	1486	1200	1654	1429
18	1762	1952	1605	1518	1709
16	511	1617	1304	1568	1250
14	1179	1337			1258
12	1500	1698	137		1112
10	1181	1170	603		985
8	1004	545	122	729	600

Table A9 lists the results (strength at break) obtained from the experiments performed to verify the new model. The columns lists the individual repetitions and the average value at the selected weight percentage polymer used.

Table A9: Results for tensile strength at break

Tensile strength (MPa)

wt% polymer	125-180µm				
	1	2	3	4	Avg
80	12.0	12.8	12.3		12.4
70	12.6	12.7	11.4		12.2
60	12.4	13.2	12.7		12.8
30	5.7	6.6	6.9	6.7	6.5
28	6.9	7.7	10.7	8.9	8.5
26	3.9	4.5	4.4	4.6	4.4
24	3.9	4.5	2.5	5.0	4.0
22	7.9	8.7	9.1	6.9	8.1
20	8.6	10.1	11.4	8.0	9.0
18	7.3	9.2	6.6	4.6	6.9
16	2.8	6.4	4.4	5.6	4.8
14	3.4	3.4	4.7		5.4
12	1.9	1.8	1.9	1.2	3.4
10	3.3	1.7	2.4		2.5
8	1.9	1.4	1.9		1.5

	250-300µm				
	1	2	3	4	Avg
80	13.6	13.2	13.4		13.4
70	12.4	13.9	12.3		12.9
60	14.1	14.1	14.3		14.2
30	4.1	4.4	6.0	4.6	4.8
28	5.4	3.9	8.8	10.1	7.1
26	7.3	6.0	7.1		6.8
24	5.7	5.4	4.9	7.2	5.8
22	8.1	6.5	9.6		8.1
20	8.2	7.2	8.2	9.5	8.3
18	5.7	10.7	8.7	7.3	8.1
16	2.3	3.2	7.6	8.1	5.3
14	5.8	5.0			5.4
12	4.2	4.9	1.3		3.4
10	3.0	3.1	1.5		2.5
8	2.0	1.9	0.7	1.0	1.4